Acute HIIE elicits similar changes in human skeletal muscle mitochondrial H2O2 release, respiration, and cell signaling as endurance exercise even with less work

Acute HIIE elicits similar changes in human skeletal muscle mitochondrial H_2O_2 release, respiration and cell signaling as endurance exercise even with less work

Adam J. Trewin[1], Lewan Parker[1,2], Christopher S. Shaw[1,2], Danielle S. Hiam[1], Andrew Garnham[1,2], Itamar Levinger[1,3], Glenn K. McConell[1], Nigel K. Stepto[1,3,4]

[1]Institute of Health and Sport, and College of Sport and Exercise Science, Victoria University, Melbourne, Australia.

[2]Institute for Physical Activity and Nutrition, School of Exercise and Nutrition Sciences, Deakin University, Victoria, Australia

[3]Australian Institute for Musculoskeletal Science (AIMSS), Department of Medicine, Western Health, Melbourne Medical School, The University of Melbourne, Melbourne, VIC, Australia.

[4]Monash Centre of Health Research and Implementation (MCHRI), School of Public Health and Preventative Medicine, Monash University, Clayton, Victoria, Australia

Corresponding Author: A/Prof. Nigel K. Stepto.

College of Sport and Exercise Science, Victoria University

PO Box 14428, Melbourne, Victoria, Australia 8001

Tel. +61 3 9919 5416; E-mail. Nigel.Stepto@vu.edu.au

Running Head: Acute exercise intensity and muscle mitochondria

Keywords: exercise, muscle, mitochondria, reactive oxygen species

Abstract

It remains unclear whether high-intensity interval exercise (HIIE) elicits distinct molecular responses to traditional endurance exercise relative to the total work performed. We aimed to investigate the influence of exercise intensity on acute perturbations to skeletal muscle mitochondrial function (respiration and reactive oxygen species), metabolic and redox signaling responses. In a randomized, repeated measures crossover design, eight recreationally active individuals (24 ± 5 years; VO_{2peak} 48 ± 11 $mL.kg^{-1}.min^{-1}$) undertook continuous moderate-intensity (CMIE: 30 min, 50% peak power output [PPO]), high-intensity interval (HIIE: 5x4 min, 75% PPO, work-matched to CMIE), and low-volume sprint interval (SIE: 4x30 s) exercise, ≥7 days apart. Each session included muscle biopsies at baseline, immediately and 3 h post-exercise for high-resolution mitochondrial respirometry (JO_2) and H_2O_2 emission (JH_2O_2), gene and protein expression analysis. Immediately post-exercise and irrespective of protocol, JO_2 increased during complex I+II leak/state-4 respiration but JH_2O_2 decreased (p<0.05). AMP-activated protein kinase (AMPK) and acetyl co-A carboxylase (ACC) phosphorylation increased ~1.5 and 2.5-fold respectively, while thioredoxin-reductase-1 protein abundance was ~35% lower after CMIE vs. SIE (p<0.05). At 3 hours post-exercise, regardless of protocol, JO_2 was lower during both ADP-stimulated state-3 OXPHOS and uncoupled respiration (p<0.05) but JH_2O_2 trended higher (p<0.08); *PPARGC1A* mRNA increased ~13-fold, and peroxiredoxin-1 protein decreased ~35%. In conclusion, intermittent exercise performed at high intensities has similar dynamic effects on muscle mitochondrial function compared with endurance exercise, irrespective of whether total workload is matched. This suggests exercise prescription can accommodate individual preferences while generating comparable molecular signals known to promote beneficial metabolic adaptations.

250 words

INTRODUCTION

Exercise is a front line strategy for the improvement of metabolic health and the prevention of numerous chronic diseases (21). Therefore, it is of clinical and public health relevance to understand the efficacy of various exercise modalities. Whether high intensity interval exercise (HIIE) elicits similar or even greater beneficial metabolic adaptations than traditional endurance type exercise remains unclear. In particular, there are conflicting reports regarding whether skeletal muscle metabolic perturbations and consequent adaptive responses are proportional to the intensity of an exercise bout when total work performed is controlled (3, 12, 18, 40). Moreover, the precise mechanisms that underlie these adaptive responses remain incompletely understood.

Increases in content and/or respiratory function of skeletal muscle mitochondria represent an important adaptive response to regular aerobic exercise training (16). Despite this, the acute effects of a single bout of exercise on mitochondrial function remain relatively less studied. Mitochondrial bioenergetics (i.e. rates of ATP synthesis via oxidative phosphorylation) are regulated in response to exercise induced perturbations (i.e. pO_2, pH, Ca^{2+}, ATP and NADH status). This can occur via complex cellular signaling events, activity of rate-limiting enzymes such as pyruvate dehydrogenase upstream of the mitochondrial electron transport system (ETS), and conceivably also by post-translational modifications to ETS proteins, although the latter has not specifically been demonstrated under exercise conditions (7, 28, 33). The mitochondrial ETS also intrinsically generates reactive oxygen species (ROS) in the form of the superoxide anion ($O_2{\cdot}^-$), which is dismutated spontaneously or more rapidly by superoxide dismutase (SOD) to hydrogen peroxide (H_2O_2) (46). The main sites of $O_2{\cdot}^-/H_2O_2$ generation during exercise are considered to be of non-mitochondrial origin such as NADPH oxidase and xanthine oxidase (49, 55, 71), yet under basal conditions

mitochondria are a primary source of $O_2\cdot^-/H_2O_2$ (24, 55). Therefore, as the skeletal muscle cellular environment returns towards basal conditions during recovery from acute exercise, mitochondria may not only rapidly revert back to being the primary source of $O_2\cdot^-/H_2O_2$, but additionally have altered rates of $O_2\cdot^-/H_2O_2$ generation. We recently reported altered skeletal muscle mitochondrial respiratory function immediately post-exercise in well trained humans (37) as well as altered post-exercise mitochondrial H_2O_2 emission in humans who are obese (66). However, to our knowledge, no study has investigated the acute effects of exercise intensity on mitochondrial function in human skeletal muscle. It is conceivable that differential mitochondrial responses to acute exercise may occur depending on intensity, since higher exercise intensity requires recruitment of a greater proportion of fast-twitch muscle fibers, whose mitochondria have been shown to have distinct functional characteristics (1).

The physiological implications of altered mitochondrial respiration and ROS emission in the hours post-exercise, are that numerous exercise-mediated adaptive responses in muscle are known to be redox-sensitive (31, 53, 57, 67). Redox sensitive signal transducers include p38 mitogen activated protein kinase (MAPK) and AMP-activated protein kinase (AMPK) (19, 29, 30). These can promote mitochondrial biogenesis signaling via peroxisome proliferator-activated receptor gamma co-activator 1-alpha (PGC1α; encoded by the gene *PPARGC1A*) (4, 60) as well as the upregulation of antioxidant capacity via transcription factors such as nuclear factor erythroid 2-related factor 2 (NRF2, encoded by the gene *NFE2L2*) (15). Downstream transcriptional targets of NRF2 include genes that encode enzymes critical for cellular redox homeostasis including SOD, glutathione peroxidase (GPX), thioredoxin (TRX), peroxiredoxin (PRDX) and thioredoxin reductase (TXNRD) (15). Additional regulation of post-exercise mitochondrial $O_2\cdot^-/H_2O_2$ generation may occur via

mitochondrial membrane remodelling processes (fission and fusion) via dynamin-related protein 1 (DRP1) and mitofusin (MFN2), respectively (2, 52); along with uncoupling protein-3 (UCP3), which, upon activation can dissipate inner mitochondrial membrane potential to mitigate $O_2{\cdot}^-/H_2O_2$ generation (41). Taken together, altered patterns of mitochondrial $O_2{\cdot}^-/H_2O_2$ emission may have important downstream effects on a range of redox-sensitive adaptive processes in the hours following exercise (31).

Therefore, the aim of this study was to test the hypothesis that when total work performed is accounted for, higher exercise intensity leads to greater post-exercise perturbations to skeletal muscle mitochondrial function (respiration and H_2O_2 emission), along with gene and protein responses related to key metabolic adaptations and redox homeostasis in young, healthy humans.

METHODS

Participants

Eight young, healthy and recreationally active individuals (six males, two females) participated in this study (mean ± SD: age 24.5 ± 5.5 yrs.; height 179 ± 8 cm; weight 79.4 ± 6.0 kg; BMI 24.8 ± 2.7 $kg{\cdot}m^{-2}$; VO_{2peak} 48.4 ± 11.2 $ml.kg^{-1}.min^{-1}$) as reported recently (50, 51). All volunteers provided written informed consent after screening for contraindications to exercise via a health assessment questionnaire. Potential participants for this study were excluded if they were currently smoking, had musculoskeletal or other conditions that prevented daily activity, symptomatic or uncontrolled metabolic or cardiovascular disease, or (females) taking oral contraception. This study was approved by and conducted in accordance with the Victoria University Human Research Ethics Committee.

Experimental Design

Participants visited the Victoria University exercise physiology laboratory on four occasions. An initial visit involved screening and a graded cycling exercise test to determine $\dot{V}O_{2peak}$ and subsequent exercise workloads to which participants were then familiarized. Three experimental trials were then conducted using a crossover study design. Trial order was randomized using the Microsoft Excel list randomize function. Trials were conducted 7-14 d apart for males, and 28 d apart for females during the early follicular phase of the menstrual cycle to control for ovarian hormone fluctuations. In each of the three experimental trials, muscle biopsy samples were collected at baseline (BASE), immediately post exercise (EX); and 3 h post-exercise (3HR).

Dietary and exercise control

Participants reported to the laboratory in an overnight-fasted state. Participants recorded all food consumed in that 24 h period in a food diary and abstained from alcohol and caffeine for 48 h and structured exercise for 24 h before each experimental trial. Photocopies of the food diary were returned to participants who were instructed to replicate this diet for the second and third visits. One litre of drinking water was provided *ad libitum* to be consumed during and after exercise, but matched between trials.

Exercise protocols

All exercise sessions were performed on an electrically braked Velotron cycle ergometer (Racermate, Seattle, WA). Participants initially performed a graded exercise test (GXT) protocol to determine peak power output (PPO) and peak oxygen uptake ($\dot{V}O_{2peak}$). Briefly, the test started at 50 W and increased by 25 W each minute until perceived exhaustion was achieved as indicated by volitional cessation of cycling, or a pedalling

cadence decreasing to below 60 rpm despite strong verbal encouragement. PPO was defined as the final complete stage, plus the fraction of the incomplete stage (26). Expired gases were collected throughout the test, and VO_{2peak} was determined with an on-line gas collection system (Moxus Modular VO_2 System, AEI Technologies, Pittsburgh, PA) calibrated as per the manufacturer's instructions. Heart rate was measured using a Polar heart rate monitor (Polar Electro, Finland). In the same visit after adequate recovery, participants were then familiarized with the experimental trial exercise protocols and workloads. One of the three exercise sessions were performed in each experimental trial. The continuous moderate-intensity exercise (CMIE) was performed at 50% of PPO for 30 min. The high-intensity interval exercise (HIIE) protocol consisted of 5 x 4 min intervals at 75% PPO interspersed with 1 min passive recovery and was matched for the total kilojoules of work performed in the CMIE protocol. The sprint exercise session (SIE) consisted of 4 x 30 s maximal sprint cycling efforts, with 4.5 min passive recovery intervals. The SIE session was not matched to CMIE/HIIE because it would be unrealistic for participants to perform an equal volume of sprint exercise given its physical demand. For the SIE exercise session, pedalling resistance was determined as a torque factor relative to body mass, optimized during the familiarisation session to achieve a pedalling cadence throughout each interval of approximately 100-120 rpm at the beginning of the 30 s bout without decreasing below ~ 40 - 50 rpm at the end. Verbal encouragement was given throughout.

Muscle biopsy sampling

Muscle samples were obtained from the middle third of the *vastus lateralis* muscle using the percutaneous needle biopsy technique as previously described (51). Briefly, after injection of a local anaesthetic into the skin and fascia (1% Xylocaine, Astra Zeneca, Australia), a small incision was made and a muscle sample taken (~120 mg) using a

Bergström biopsy needle with suction. Each biopsy was taken from a separate incision ~1 cm proximal from the previous biopsy. Muscle samples were dissected free of any visible connective tissue then one portion frozen in liquid nitrogen and stored at -80 °C, and another placed in ice-cold BIOPS preserving solution for mitochondrial functional analyses (see below).

Preparation of permeabilized muscle fibers

To 'capture' the acute regulatory effects of exercise on mitochondrial function, immediately after the biopsy, muscle fiber bundles were placed into ice-cold preserving solution (BIOPS; containing in mM: 7.23 K_2EGTA, 2.77 CaK_2EGTA, 5.77 Na_2ATP, 6.56 $MgCl_2$-$6H_2O$, 20 taurine, 15 phosphocreatine, 20 imidazole, 0.5 dithiothreitol, 50 K^+-MES; pH 7.1) then prepared as per our previous work (66). Briefly, a small portion of muscle fibers were mechanically separated then transferred to ice-cold BIOPS supplemented with saponin (50 µg/mL) for 30 min with agitation. This was followed by agitation in ice-cold respiration buffer (MiR05; in mM: 0.5 EGTA, 10 KH_2PO_4, 3 $MgCl_2$-$6H_2O$, 60 lactobionic acid, 20 taurine, 20 HEPES, 110 D-sucrose, 1 mg/mL bovine serum albumin; pH 7.1). Two portions of the fiber bundles were blotted on filter paper for 5 s, and wet-weight (ww) mass was recorded using a microbalance (3 – 4 mg-ww per replicate).

Mitochondrial respiration and hydrogen peroxide emission assay

To determine mitochondrial function and concomitant ROS emitting potential in the form of H_2O_2 (JH_2O_2), permeabilized muscle fiber bundles were assessed in duplicate using a high resolution respirometer (Oxygraph O2k, Oroboros Instruments, Innsbruck, Austria) in respiration buffer MiR05 as per our previous work (62, 66). Briefly, a substrate, uncoupler, inhibitor titration (SUIT) protocol was performed at 37ºC with O_2 concentration maintained

between 300-500 *n*mol.ml^{-1}. Specifically, sequential titrations of substrates were added firstly to assess mitochondrial Complex I leak ($LEAK_{CI}$) with malate (2 mM) and pyruvate (10 mM), followed by succinate (10 mM) to assess Complex II ($LEAK_{CI+II}$) state 4 respiration. Oxidative phosphorylation (state 3 respiration) supported by CI+II substrates ($OXPHOS_{CI+II}$) was then determined with titrations of adenosine diphosphate (ADP) at 0.25, 1 and 5 mM; the latter being considered a saturating concentration since it did not lead to significantly greater JO_2 rates compared with 1 mM. Cytochrome *c* (10 µM) was added to confirm membrane integrity (< 15% increase in O_2 flux), then peak uncoupled respiratory flux was measured after 2-4 titrations of 25 nM carbonyl cyanide *p*-trifloromethoxyphenylhydrazone (FCCP) to assess maximal capacity of the electron transfer system supported by convergent CI and CII substrate input (ETS_{CI+II}). Inhibitors of specific complexes were then applied: rotenone (1 µM) to inhibit CI resulting in ETS supported only by CII substrate flux (ETS_{CII}), followed by the CIII inhibitor antimycin A (5 µM) to determine background O_2 flux. These JO_2 values were subtracted from all prior measures to account for any artefactual non-ETS O_2 consumption (mean ± SD across all experiments: 3.86 ± 1.39 *p*mol.s^{-1}.mg-ww^{-1}). Measurements of oxygen fluxes were averaged from both chambers during steady-state for each respiratory state. If one of the chambers did not reach steady state flux, that value was excluded from the analysis of that respiratory state. Throughout the respiration protocol, rates of H_2O_2 emission were simultaneously assessed via the Amplex UltraRed (25 µM; Molecular Probes, Invitrogen) and horseradish peroxidase (2.5 U.mL^{-1}) reaction with H_2O_2 in the presence of added superoxide dismutase (SOD; 2.5 U.mL^{-1}). The formation of the fluorescent reaction product (resorufin) was measured via excitation/emission at 525/600 *nm* (Oroboros O2k-Fluorescence LED-2 Module, Anton Paar, Graz, Austria) (27, 34). Signal was calibrated at the beginning of each experiment with 40 nM titrations of H_2O_2 and expressed relative to sample mass (mg.wet-weight^{-1}).

Real-time quantitative polymerase chain reaction

RNA was isolated from BASE and 3HR muscle samples by mechanical homogenization (Tissuelyser, Qiagen, Australia) with Tri reagent, followed by 1-bromo-3-chloropropane and isopropanol precipitation (Sigma Aldrich, Castle Hill, NSW, Australia), which was then dissolved in DNase and RNase free water. RNA samples were tested spectrophotometrically (Bio-Photometer, Eppendorf, Germany) for concentration at 260 nm and quality, indicated by the 260:288 nm absorbance ratio (mean ± SD: 2.15 ± 0.18). One microgram of RNA was then reverse transcribed to cDNA (iScript kit, BioRad, Gladesville NSW, Australia). Real-time qPCR reactions were carried out in a Mastercycler RealPlex 2 (Eppendorf, Hamburg, Germany) with Taq enzyme reagent (iTaq SYBR Green, BioRad, Gladesville NSW, Australia) and forward and reverse primers (Sigma Aldrich, Castle Hill, NSW, Australia) for target mRNAs, which were generated from the NCBI Primer-BLAST database as shown in Table 1. The conditions for RT-qPCR were an initial 3 min annealing phase at 95ºC, then 40 cycles of 15 s at 95ºC and 1 min at 60ºC. Following this, a 20 min melting curve (60ºC to 95ºC) was performed to confirm the amplification of a single product. Cycle thresholds (C_T) were calculated using software (RealPlex, Eppendorf) and used to quantify mRNA expression via the $-2\Delta\Delta C_T$ method (39) normalized to a housekeeping gene, β2 microglobulin (*β-2M*).

Muscle protein extraction and western blotting

Frozen muscle was processed for western blotting as per our previous work (66). Protein (6-8 µg per lane) was then loaded into precast 26 well stain-free 4-20% gradient gels (Criterion™ TGX Stain-Free™ Precast, BioRad, Gladesville NSW, Australia) along with molecular weight ladder (PageRuler® Plus, Thermo Scientific, Australia) and pooled sample.

The pooled sample was made by combining small volumes of all samples into a single pooled sample and used to construct a five-point standard curve (2 to 16 µg protein) on all gels to allow direct comparison of blot intensities via linear regression, as described in detail elsewhere (47). Stain-free gels were activated by UV light (ChemiDoc™ MP, BioRad, Gladesville NSW, Australia) and imaged to visualize the total protein of each lane. Proteins were then transferred to PVDF membranes (Trans-Blot® Turbo™, BioRad, Gladesville NSW, Australia), blocked, and then incubated overnight at 4ºC with the following primary antibodies diluted 1:1000 in TBST containing 5% BSA and 0.1% sodium azide: anti-phospho-Acetyl Co-A carboxylase (p-ACCβ^{Ser221}, Cell Signaling #11818), anti-phospho AMP-activated protein kinase (p-AMPK^{Thr172}, Cell Signaling #2531), anti-Dynamin Related Protein 1 (DRP1, Cell Signaling #5391), anti-Glutathione (Abcam #19534), anti-Glutathione Peroxidase 1 (GPX1, Cell Signaling #3286), anti-phospho heat shock protein 27 (p-HSP27^{ser82}, Enzo ADI-SPA-524), Anti-Heat shock protein 72 (HSP72; Enzo ADI-SPA-810), Mitoprofile cocktail (MitoSciences #MS601, consisting of anti-complex I subunit NDUFB8 [complex-I, Abcam #110242], anti-complex II subunit 30kDa [complex-II, Abcam #14714], anti-complex III subunit core 2 [complex-III, Abcam #14745], anti-complex IV subunit II [complex-IVs2, Abcam #110258], and anti-ATP synthase subunit alpha [complex-V, Abcam #14748]), anti-complex IV subunit IV (complex-IVs4, Mito Sciences #MS407), anti-Mitofusin 2 (MFN2; Cell Signaling #9482), PRDX pathway cocktail (Abcam #184868, consisting of anti-Peroxiredoxin 1 [PRDX1], anti-Thioredoxin [TRX], and anti-Thioredoxin reductase-1 [TXNRD1]), anti-PPARγ coactivator-1α (PGC1α, Cell Signaling #2178), anti-Mitochondrial Transcription Factor 1 (TFAM, Abcam #475017), anti-uncoupling protein 3 (UCP3, Abcam #10985). Membranes were then probed with appropriate horseradish peroxidase-conjugated secondary antibody (PerkinElmer, Glen Waverly, Victoria, Australia), at a dilution of 1:50,000 – 100,000 in 5% non-fat milk TBST for 1 hr at room temperature.

ECL (SuperSignal® West Femto, Thermo Scientific, Australia) was applied for imaging with a high sensitivity CCD camera (ChemiDoc™ MP, BioRad, Gladesville NSW, Australia) and subsequent analysis was performed (ImageLab v 5.1, BioRad, Gladesville NSW, Australia). Total protein loading of each sample was determined from stain-free images of each gel and these values were then used to normalize each protein of interest after normalization to its standard curve.

Co-immunoprecipitation of glutathionylated proteins

Frozen muscle was sectioned and homogenized as described above, but with 200 µL non-denaturing lysis buffer (20 mM Tris HCl pH 8; 137 mM NaCl; 1% Triton X-100; 2 mM EDTA; 1% v/v protease inhibitor cocktail [Sigma Aldrich]; and 25 mM N-ethylmalemide). Muscle lysate (50 µg protein) was added to 100 µL washed protein-A sepharose beads (GE Health/Amersham Biosciences), with 1 µL anti-glutathione primary antibody (Abcam #19534) which was incubated for 4 h at 4ºC with rotation. Antigen-antibody-bead conjugates were centrifuged and supernatant discarded (supernatant was tested for efficacy of IP pull-down during optimisation), followed by a further 3 washes. Subsequently, 50 µL denaturing lysis buffer (125 mM Tris-HCl, 4% SDS, 10% Glycerol, 10 mM EGTA, 100 mM DTT) was added to the bead-protein-antibody conjugate, then heated at 95ºC for 5 min to elute proteins from the bead-antibody conjugate. Bromophenol blue dye (1% v/v) was added before performing SDS-PAGE and immunoblotting as described above with the Mitoprofile cocktail (MitoSciences #MS601) and UCP3 (Abcam #10985) antibodies.

Statistical analysis

Data were analysed by one-way (exercise-intensity) or two-way (exercise-intensity x time) ANOVA with repeated measures where appropriate (SPSS Statistics, IBM v1.0.0.642).

Mauchly's test of sphericity was performed and Greenhouse-Geisser correction applied where non-sphericity was detected. Where significant main interaction, time, or exercise-intensity effects were detected, post hoc analyses were conducted with Bonferroni correction for multiple comparisons. Statistical significance was accepted at $p<0.05$, and trends indicated at $p\leq0.10$. Where significant main effects were detected, effect sizes (ES) were calculated on data pooled from all three exercise protocols for pairwise comparison between time points using Cohen's *d* with 95% lower to upper confidence intervals (CI), without correction for multiple comparisons. Data are reported as mean ± SD for $n=8$ unless otherwise stated.

RESULTS

Physiological responses to exercise

Total external work of work-matched CMIE and HIIE was 4-fold greater than SIE (Table 2). Greater exercise intensity increased rating of perceived exertion (SIE > HIIE > CMIE, $p<0.001$), despite HIIE leading to the highest HR_{peak} ($p<0.001$, Table 2).

Mitochondrial respiration

State-4 leak respiration supported by complex-I ($LEAK_{CI}$) or I+II ($LEAK_{CI+II}$) substrates was not differentially affected by exercise intensity, but increased with time by 65% ($p=0.003$; ES 1.34, 95% CI 1.03 to 1.65; Figure 1B) and 40% ($p<0.001$; ES 0.77, 95% CI 0.59 to 0.95; Figure 1C) respectively, in a BASE vs. EX comparison across all exercise protocols. At 3HR, $LEAK_{CI}$ remained ~30% elevated above BASE ($p<0.047$; ES 0.57, 95% CI 0.33 to 0.82). State-3 oxidative phosphorylation (5 mM ADP) supported by complex I+II ($OXPHOS_{CI+II}$) was not affected by exercise intensity (*exercise-intensity x time*, $p=0.154$), but

was ~15% lower at 3HR compared with EX across all exercise protocols (p=0.003; ES -0.27, 95% CI -0.44 to -0.10; Figure 1D). Uncoupled respiration (with FCCP) supported by complex I+II (ETS_{CI+II}), or II only (plus rotenone) was not affected by exercise intensity, but was 15% (p=0.009; ES -0.35, 95% CI -0.53 to -0.16; Figure 1E) and 30% (p=0.024; ES -0.52, 95% CI -0.81 to -0.24; Figure 1F) lower, respectively, at 3HR compared with EX across all exercise protocols. The JO_2 ratio between 0.25 v.s. 5 mM ADP under $OXPHOS_{CI+II}$ conditions was not significantly affected by exercise protocol or time (data not shown).

Mitochondrial H_2O_2 emission

During both complex-I ($LEAK_{CI}$) and I+II ($LEAK_{CI+II}$) supported leak respiration, JH_2O_2 was not affected by exercise intensity, but was elevated ~55% during $LEAK_{CI}$ at 3HR relative to EX across all exercise protocols (p=0.018; ES 0.94, 95% CI 0.55 to 1.33; Figure 2B). In contrast, during $LEAK_{CI+II}$, JH_2O_2 was ~30% lower at EX (p=0.008; ES -0.83, 95% CI -1.08 to -0.57), and ~40% lower at 3HR (p<0.001; ES -0.97, 95% CI -1.22 to -0.72; Figure 2C) relative to BASE across all exercise protocols. During complex I+II supported state-3 oxidative phosphorylation respiration ($OXPHOS_{CI+II}$), JH_2O_2 was unaffected by exercise intensity, but tended to be elevated ~65% at 3HR relative to EX across all protocols (p=0.057; ES 0.71, 95% CI 0.32 to 1.10; Figure 2D). Similarly, during uncoupled respiration (plus FCCP) supported by complex I+II substrates (ETS_{CI+II}) there was no effect of exercise intensity on JH_2O_2 but this tended to be increased by ~95% (p=0.072; ES 0.63, 95% CI 0.26 to 0.99; Figure 2E) at 3HR compared to EX across all protocols. However, JH_2O_2 was unaffected by exercise during uncoupled respiration supported by complex-II only (plus rotenone), (Figure 2F). Expressed as a ratio relative to JO_2, JH_2O_2 was lower in $LEAK_{CI}$ at EX vs. BASE (p=0.030; ES 1.01, 95% CI -1.47 to -0.54), but during all other respiratory states the overall effects of exercise on this ratio closely reflected absolute JH_2O_2 rates.

346

347 **Protein phosphorylation responses to exercise**

348 There were no effects of exercise intensity on phosphorylation of AMPK^{Thr172}
349 (p=0.197), ACCβ^{Ser221} (p=0.490), or HSP27^{Ser82} (p=0.568); however, each of these increased
350 by ~1.5 fold (p=0.001; ES 0.86, 95% CI 0.52 to 1.19; Figure 3B), ~2.5 fold (p<0.001; ES
351 2.15, 95% CI 1.68 to 2.62; Figure 3C) ~2.5 fold (p=0.051; ES 1.09, 95% CI 0.62 to 1.57;
352 Figure 3D) across all exercise protocols at EX relative to BASE, respectively.

353

354 **Exercise and redox sensitive gene expression**

355 There were no significant effects of exercise intensity, however there were main
356 effects for increased skeletal muscle mRNA levels of *PPARGC1A* (p=0.027; ES 0.86, 95%
357 CI 0.47 to 1.25), *UCP3* (p=0.027; ES 0.70, 95% CI 0.31 to 1.09), *BNIP3* (p=0.010; ES 0.48,
358 95% CI 0.09 to 0.88) and *PRDX1* (p=0.034; ES 0.36, 95% CI -0.12 to 0.83) at 3HR relative
359 to BASE across all exercise protocols (Figure 4 A and B). There were trends for increases in
360 *MFN2* (p=0.057; ES 0.37, 95% CI -0.03 to 0.76), *DRP1* (p=0.091; ES 0.45, 95% CI 0.06 to
361 0.85), *GPX1* (p=0.092; ES 0.58, 95% CI 0.19 to 0.98) and *TXNRD1* (p=0.069; ES 0.43, 95%
362 CI 0.04 to 0.82) mRNA levels at 3HR compared with BASE across all protocols, while there
363 were no main effects of time on *NFE2L2* (p=0.427) or *SOD1* (p=0.282) or *SOD2* mRNA
364 (p=0.186; Figure 4B).

365

366 **Skeletal muscle antioxidant and mitochondrial protein abundance**

367 Overall, we found no effect of time nor exercise intensity in the expression levels of
368 key antioxidant enzymes TRX and GPX1, the chaperone HSP72, mitochondria related
369 proteins MFN2, DRP1, PGC1α (Figure 5) or complexes I-V (Figure 6). However, there was
370 significantly decreased abundance of PRDX1 by ~-35% (p=0.033; ES -0.69, 95% CI -0.95 to

-0.44; Figure 5B), TFAM by ~15% (p=0.007; ES -0.34, 95% CI -0.54 to -0.14; Figure 5J) and a tendency for lower UCP3 by ~20% (p=0.078; ES -0.56, 95% CI -0.82 to -0.30; Figure 5I) at 3HR compared with BASE across all exercise protocols. There was a significant main interaction effect of *exercise intensity x time* on thioredoxin reductase (TXNRD1) protein abundance (p=0.032). Specifically, at EX, there was ~35% less TXNRD1 protein detected following the CMIE protocol compared with the SIE protocol (p=0.007; ES -0.72, 95% CI -1.33 to -0.10; Figure 5E).

Mitochondrial protein S-glutathionylation

No significant effects of exercise were found for S-glutathionylation of mitochondrial proteins ATP-synthase-α (p=0.975), Complex-IV^{subunit2} (p=0.931), or UCP3 (p=0.668; Figure 7).

DISCUSSION

The present study design allowed for a direct within-subject comparison of mitochondrial responses to acute bouts of CMIE and HIIE on a work-matched basis, as well as comparisons of these with low-volume sprint interval exercise (~25% of the total work volume of CMIE/HIIE) in young healthy humans. The main findings were that regardless of the exercise protocol performed, peak mitochondrial H_2O_2 emission (during non-phosphorylating complex-I+II supported respiration) was lower immediately post-exercise, yet rates of mitochondrial H_2O_2 emission tended to be elevated three hours later during complex-I+II supported ADP-stimulated oxidative phosphorylation and also uncoupled respiratory states. These acute changes in mitochondrial oxidant emission occurred concomitantly with increases in mitochondrial oxygen consumption rates during non-

phosphorylating respiratory states immediately post-exercise, yet three hours post-exercise oxygen consumption was lower during oxidative phosphorylation and uncoupled respiratory rates. Consistent with these acute mitochondrial responses to exercise, a range of key muscle metabolism-related protein phosphorylation events, as well as gene and protein expression of putative redox-sensitive targets generally increased to equivalent levels in the early post-exercise period regardless of protocol.

In the present study, higher exercise intensity had more pronounced effects on systemic physiologic responses as indicated via session HR_{peak} and RPE, in addition to blood lactate, glucose, and activity of specific stress-activated protein kinases, recently reported elsewhere (50, 51). Despite this, we found no exercise protocol-dependent effects on mitochondrial parameters. To establish where these divergent responses to different exercise protocols occurred (i.e. only at the mitochondria or also at the whole muscle level), we assessed key molecular markers of skeletal muscle energy metabolism and overall stress induced by the exercise protocols. Intriguingly, phosphorylation of $AMPK^{Thr172}$ (indicative of cellular bioenergetic perturbation) increased to a similar degree regardless of exercise protocol, as did its downstream substrate $ACC\beta^{Ser221}$. Furthermore, mRNA expression of *PPARGC1A*, the gene encoding PGC1α, and a target of AMPK signaling, increased ~13 fold at 3HR, regardless of exercise protocol. Previously, Egan *et al.* (18) reported that high intensity continuous exercise generated greater mitochondrial biogenesis signaling than work-matched moderate intensity continuous exercise. A possible explanation for this is the longer exercise duration and that the lowest exercise intensity protocol employed in that study (18) was 40% $\dot{V}O_{2peak}$, whereas the lowest in the present study was ~55% $\dot{V}O_{2peak}$. Indeed, the 3 h post-exercise increases in *PPARGC1A* mRNA expression, p-AMPK and p-ACC in all intensities of the present study is similar to what was reported for their HIIE (80%

419 $\dot{V}O_{2peak}$) exercise. In support of this notion, Chen *et al.* (8) demonstrated that AMPK
420 phosphorylation only occurred following exercise at 60% $\dot{V}O_{2peak}$ and above, but not at 40%
421 $\dot{V}O_{2peak}$. Recently, a well-designed study by MacInnis *et al.* (40) compared training responses
422 to single-leg cycling CMIE in one leg and HIIE matched for both work and duration in the
423 opposite leg. They reported superior mitochondrial adaptations (assessed via increased citrate
424 synthase activity and mitochondrial respiratory rates) following HIIE training, although this
425 occurred in a fiber-type dependent manner (40), the effects of which are likely an important
426 factor in the long-term response to training (38). It is possible that there were additional
427 factors not controlled for in the present study that may contribute to a greater response to
428 repeated bouts (i.e. training) of HIIE compared to CMIE, such as number of transitions
429 between work and rest (10). Nevertheless, our findings are consistent with other studies
430 comparing HIIE to CMIE, that have reported equivalent, but not greater adaptive responses
431 when matched for total work performed (3, 72). Interestingly, we also found that SIE led to
432 equivalent mitochondrial and signaling responses as the CMIE and HIIE, despite consisting
433 of considerably less total work. This suggests that the stimulus provided by each of the
434 exercise protocols in the present study reached a threshold at least sufficient for activation of
435 the assessed signaling pathways in muscle. Indeed, this is in line with earlier findings
436 demonstrating the efficacy of low volume SIE (5, 22, 25). However, the complexity of the
437 molecular signals generated and transduced in response to exercise should not be understated,
438 since other signaling pathways can be differentially activated to ultimately elicit specific
439 training adaptations to distinct exercise modalities (51). Taken together, our findings
440 nevertheless support the notion that similarly robust molecular signals can be generated in
441 skeletal muscle in response to a broad range of exercise stimuli.

Relatively few studies have investigated acute post-exercise changes in mitochondrial function. Given that $O_2^{\cdot -}/H_2O_2$ generation is intrinsically linked to the respiratory state (11), the present findings of altered mitochondrial H_2O_2 emission in the hours post-exercise in a respiratory state-dependent manner is consistent with previous reports from our group and others showing that exercise acutely alters mitochondrial respiration (37, 63, 64, 66). Despite the lack of effect of exercise intensity, there was a robust and dynamic effect of acute exercise on mitochondrial function, such as decreasing post-exercise JH_2O_2 during the succinate driven $LEAK_{CI+II}$ respiration state. Succinate-driven JH_2O_2 formation occurs primarily via superoxide generation due to reverse electron flow through the flavin mononucleotide site in complex-I under experimental conditions of high inner mitochondrial membrane potential in the absence of ADP (46). Conceivably, high membrane potential could occur during situations of prolonged low ATP demand (24) such as with physical inactivity and sedentary lifestyle. Our findings therefore suggest a mechanism by which exercise may decrease JH_2O_2 in the post-exercise 'basal' respiratory state. This may be pertinent for attenuation of oxidative stress that has been associated with various pathophysiologic states including insulin resistance (32).

The decreased post-exercise H_2O_2 emission under reverse electron flow mitochondrial respiratory conditions may be attributed to increased proton leak (i.e. uncoupling) at the inner mitochondrial membrane in response to exercise. This is supported by our finding of simultaneously increased post-exercise O_2 flux under the same $LEAK_{CI+II}$ respiratory state, and is consistent with findings from an earlier study using permeabilized muscle mitochondria in young, healthy humans (63). The increased post exercise mitochondrial membrane proton leak would also decrease proton-motive force available to drive ATP synthesis. This supports our observation of lower state-3 ADP stimulated oxidative-

phosphorylation (*OXPHOS*) respiration at three hours post-exercise, and is comparable to the changes observed in permeabilized muscle mitochondria following high-intensity running in horses (69). One previous study in humans reported no change in *OXPHOS* JO_2 following exhaustive human exercise (64). However, their measurements were made under conditions where the flux of substrates through the ETS would be submaximal, since only complex-I substrates were used with no convergent electron input from the complex-II substrate succinate, likely masking any effect of exercise on maximal *OXPHOS* activity. It should be noted, however, that we cannot exclude the potential contribution of pyruvate dehydrogenase activity, which is well known to be regulated by exercise (54). Given that we used pyruvate as the sole complex-I substrate, this may affect substrate availability for complex-I in our experimental system. Nevertheless, during this $OXPHOS_{CI+II}$ respiratory state, we found a trend for elevated JH_2O_2 at 3 h post exercise and a significant elevation with uncoupled ETS_{CI+II}. This is despite the ETS functioning in the 'normal' forwards direction under these respiratory states (i.e. any $O_2{\cdot}^-/H_2O_2$ formed not via reverse electron flow). This suggests that the elevated $O_2{\cdot}^-/H_2O_2$ formed specifically in this ADP stimulated state-3 respiratory state may be attributed to altered ETS respiratory complex activity, potentially via exercise-induced post-translational modifications. Intriguingly, the trend for elevated JH_2O_2 at 3HR during uncoupled respiration was absent after the addition of rotenone (ETS_{CII}), suggesting an effect of exercise directly or indirectly at the complex-I_Q site (74). While it should be noted that the use of inhibitors and saturating substrate concentrations used in our *ex vivo* preparation may not recapitulate the native *in vivo* cellular environment and rates of superoxide formation, these findings nonetheless highlight that acute exercise can modify a) mitochondrial inner membrane proton leak and b) ETS derived $O_2{\cdot}^-/H_2O_2$ emission characteristics in the hours post-exercise.

Mitochondrial function may be regulated by redox-mediated post translational modifications such as S-glutathionylation of cysteine residues within ETS proteins (42). To investigate this possibility in the context of exercise, we probed S-glutathionylation of mitochondrial ETS subunits including ATP-synthase subunit-α (complex-V) and cytochrome c oxidase subunit 2 (complex-IV) using the mitochondrial cocktail antibody following immunoprecipitation with anti-GSH (Figure 7). We were unable to observe any significant effects of exercise on these, possibly as a result of limited sample material only allowing for n=4. While the NDUFB8 complex-I subunit detected by the commonly used mitochondrial cocktail antibody did not display detectable levels of S-glutathionylation, other subunits of complex-I such as NDUFS7 and NDUFV1 contain iron-sulphur clusters susceptible to oxidation and are known regulators of complex-I $O_2{\cdot}^-/H_2O_2$ generation (17, 23). We also probed for S-glutathionylation of UCP3, which is known to regulate inner mitochondrial membrane potential and thereby modulate respiratory function and rates of superoxide formation (43). Although we also did not detect significant effects of exercise on this, future studies may utilize mass spectrometry to investigate these and other redox mediated post-translational protein modifications in further detail (33).

We observed a decrease in PRDX1 protein abundance in muscle at 3HR, a cytosolic protein with low K_M for H_2O_2 (i.e. scavenges low levels of H_2O_2) (6). The decreased PRDX1 abundance at 3HR could impair the scavenging of mitochondrial H_2O_2, allowing localized ROS accumulation for the induction of redox signaling. This decrease is consistent with a recent report demonstrating that peroxiredoxins are rapidly degraded by ubiquitin mediated processes after being oxidized (59). Potentially in response to this, there was a small yet significant increase in *PRDX1* mRNA levels 3 hours post-exercise, supporting the notion that the PRDX/TRX antioxidant pathway plays an important role in exercise-induced redox

signaling (70). TXNRD1 is a cytosolic protein that reduces TRX using NADPH, to in turn reduce PRDX. Interestingly, TXNRD1 protein content was lower after CMIE compared to SIE. This was the sole indication of a significant exercise protocol-dependent effect on muscle redox homeostasis in the present study. It is possible that similar mechanisms exist for the degradation of TXNRD1 similar to that of peroxiredoxins (59). We recently reported elsewhere that specific components of muscle and plasma redox homeostasis pathways were affected by exercise intensity (50). Therefore, it is tempting to speculate that different exercise protocols may exert subtle, yet important effects in fine-tuning specific aspects of muscle redox homeostasis, which warrants further investigation.

The *NFE2L2* gene encodes NRF2, a redox-sensitive transcription factor and master-regulator of the antioxidant transcriptional response (15). Although *NFE2L2* mRNA was unchanged 3 hours after exercise, it is likely that this would have peaked and returned to baseline levels before the 3HR time point (15, 48). Interestingly, downstream gene targets of NRF2 were not significantly affected by exercise: *SOD1*, *SOD2* and *GPX1* mRNA expression, although there was a small yet significant increase in *PRDX1* mRNA at 3 h post-exercise. It is possible that the exercise protocols in the present study, irrespective of work, were not sufficient for full activation of the NRF2 transcriptional response, or at least at the time points assessed. Among other putative redox and exercise sensitive responses assessed, cytosolic heat-shock protein HSP27 phosphorylation increased post-exercise as expected, while total abundance of the higher molecular weight HSP72 protein was unaffected. Previously, exercise intensity-dependent increases of HSP72 were shown in rat skeletal muscle (44) as well as 3 days after HIIE in humans (9), and this has also been shown to occur via an exercise-induced $O_2\cdot^-/H_2O_2$ pathway (58). However, numerous environmental factors and molecular signals can also induce HSP72 expression in addition to $O_2\cdot^-/H_2O_2$ (14, 56).

We observed an increase in *BNIP3* mRNA expression 3 hours post-exercise which is involved in the mitochondrial quality control processes via mitophagy (75). Mitophagy has previously been shown to be affected by exercise via both PGC1α (68) and $O_2\cdot^-/H_2O_2$ (36). Our data suggest this response is not differentially affected by exercise intensity in human muscle, consistent with many of the other mitochondrial parameters measured in this study. Also unaffected by the present exercise protocols was abundance of DRP1 and MFN2, which regulate outer mitochondrial membrane fission and fusion, respectively. MFN2 protein levels did however show a tendency to increase to a greater extent at 3 hours post-exercise with SIE compared with CMIE. This is in line with previous literature showing that MFN2 protein was unchanged after 3 h of 'low' intensity voluntary wheel running in mice (52) yet increased 3 h after 60 min of exercise at 70% $\dot{V}O_{2peak}$ in healthy middle aged humans (35). Nevertheless, it should be noted that post-exercise mitochondrial dynamics are most likely determined by acute post-translational modifications to fission/fusion proteins rather than their total abundance alone (65).

While this randomized crossover study design provided a number of novel findings, some potential limitations should also be considered. The small sample size and sex-distribution (male, *n*=6, female, *n*=2) in the present study precludes the detection of potentially subtle sex-dependent differences in responses to exercise (20). Although we tested females during the early follicular phase of the menstrual cycle to minimize the impact of ovarian hormone fluctuations, and that skeletal muscle mitochondrial respiratory function was previously shown to be equivalent between men and women (61), sex-specific effects should nevertheless be considered in future investigations. Higher intensity exercise involves the recruitment of a greater proportion of fast twitch fibers (73), however, in the present study fiber-type specific responses were not assessed which could potentially mask some exercise-

562 intensity specific effects as recently reported (40). In our mitochondrial respiration
563 experiment, addition of succinate prior to ADP in the absence of rotenone stimulates maximal
564 levels of superoxide production due to reverse electron transfer, and the effect of exercise on
565 this was a key outcome measure in the present study. However, it should be acknowledged
566 that the ROS generated in this respiratory state could influence subsequent respiratory
567 measures by altering redox sensitive components of the ETS or other proteins such as the
568 adenine nucleotide translocase (ANT). Due to limited sample material it was not possible to
569 measure cellular glutathione levels (GSH and the oxidized form, GSSG) which would have
570 been informative to understand whether the observed post exercise changes in JH_2O_2 were
571 primarily due to altered rates of ROS generation alone or whether changes in GSH mediated
572 oxidant scavenging also contributed to this effect. It is also possible that other non-ETS
573 mitochondrial enzymes not assessed in the present study could contribute to the background
574 net emission of mitochondrial H_2O_2. Lastly, it should be noted that while the Amplex
575 UltraRed assay is intended to report mitochondrial H_2O_2 emission towards the cytosol, it may
576 not be exclusive to this since the fluorescent reaction product, resorufin, has been shown to
577 interact with intracellular sources of peroxides and/or peroxynitrites (13) or carboxylesterases
578 (45). Thus, it is conceivable that this could confound absolute quantification of JH_2O_2 in the
579 present study. However, the relative changes in JH_2O_2 observed can be attributed to specific
580 ETS sites, since these effects were observed only with their respective site-specific substrate
581 and/or inhibitor combination.

582 **Perspectives and significance**

583 In conclusion, we provide novel evidence that mitochondrial function (respiration and
584 H_2O_2 emission) in human skeletal muscle are transiently altered in a respiratory state-
585 dependent manner in the hours following continuous moderate and high intensity interval

exercise irrespective of whether these exercise modes are matched for total work. Moreover, regardless of exercise protocol, there were comparable responses across a range of known and putative redox and exercise-sensitive transcriptional and protein responses. Importantly, a total of only two minutes of sprint interval exercise was sufficient to elicit similar responses as 30 minutes of continuous moderate intensity aerobic exercise. This suggests that exercise may be prescribed according to individual preferences while still generating similar signals known to confer beneficial metabolic adaptations. These findings have important implications for improving our understanding of how exercise can be used to enhance metabolic health in the general population.

Acknowledgments

We are extremely grateful for the generous efforts of the volunteers who enthusiastically participated in this study.

Current addresses:

A.J.T.: Department of Anesthesiology and Perioperative Medicine, University of Rochester Medical Center, Rochester, NY, USA.

Grants: A/Prof Nigel Stepto was supported by the Australian Governments Collaborative Research Network. A/Prof Levinger was supported by Future Leader Fellowship (ID: 100040) from the National Heart Foundation of Australia.

Disclosures: There are no conflicts of interest to declare.

REFERENCES

1. **Anderson EJ, and Neufer PD**. Type II skeletal myofibers possess unique properties that potentiate mitochondrial H2O2 generation. *American Journal of Physiology-Cell Physiology* 290: C844-C851, 2006.
2. **Archer SL, and Longo DL**. Mitochondrial dynamics—mitochondrial fission and fusion in human diseases. *New England Journal of Medicine* 369: 2236-2251, 2013.
3. **Bartlett JD, Joo CH, Jeong T-S, Louhelainen J, Cochran AJ, Gibala MJ, Gregson W, Close GL, Drust B, and Morton JP**. Matched work high-intensity interval and continuous running induce similar increases in PGC-1α mRNA, AMPK, p38, and p53 phosphorylation in human skeletal muscle. *J Appl Physiol* 112: 1135-1143, 2012.
4. **Brigelius-Flohé R, and Flohé L**. Basic principles and emerging concepts in the redox control of transcription factors. *Antioxidants & redox signaling* 15: 2335-2381, 2011.
5. **Burgomaster KA, Howarth KR, Phillips SM, Rakobowchuk M, MacDonald MJ, McGee SL, and Gibala MJ**. Similar metabolic adaptations during exercise after low volume sprint interval and traditional endurance training in humans. *J Physiol* 586: 151-160, 2008.
6. **Chae HZ, Kim HJ, Kang SW, and Rhee SG**. Characterization of three isoforms of mammalian peroxiredoxin that reduce peroxides in the presence of thioredoxin. *Diabetes research and clinical practice* 45: 101-112, 1999.
7. **Chen C-L, Varadhara S, Kaumaya PP, Zweier JL, and Chen Y-R**. Oxidative modification with protein tyrosine nitration occurs following deglutathiolation of the 70 kDa flavoprotein of mitochondrial complex II is associated with loss of electron transfer activity in the post-ischemic myocardium. *Circulation* 118: S_273, 2008.
8. **Chen Z-P, Stephens TJ, Murthy S, Canny BJ, Hargreaves M, Witters LA, Kemp BE, and McConell GK**. Effect of exercise intensity on skeletal muscle AMPK signaling in humans. *Diabetes* 52: 2205-2212, 2003.
9. **Cobley JN, Sakellariou GK, Owens D, Murray S, Waldron S, Gregson W, Fraser W, Burniston JG, Iwanejko LA, and McArdle A**. Lifelong training preserves some redox-regulated adaptive responses after an acute exercise stimulus in aged human skeletal muscle. *Free Radic Biol Med* 70: 23-32, 2014.
10. **Combes A, Dekerle J, Webborn N, Watt P, Bougault V, and Daussin FN**. Exercise-induced metabolic fluctuations influence AMPK, p38-MAPK and CaMKII phosphorylation in human skeletal muscle. *Physiological reports* 3: 2015.
11. **Cortassa S, O'Rourke B, and Aon MA**. Redox-optimized ROS balance and the relationship between mitochondrial respiration and ROS. *Biochimica et Biophysica Acta (BBA)-Bioenergetics* 1837: 287-295, 2014.
12. **Daussin FN, Zoll J, Dufour SP, Ponsot E, Lonsdorfer-Wolf E, Doutreleau S, Mettauer B, Piquard F, Geny B, and Richard R**. Effect of interval versus continuous training on cardiorespiratory and mitochondrial functions: relationship to aerobic performance improvements in sedentary subjects. *American Journal of Physiology-Regulatory, Integrative and Comparative Physiology* 295: R264-R272, 2008.
13. **Dębski D, Smulik R, Zielonka J, Michałowski B, Jakubowska M, Dębowska K, Adamus J, Marcinek A, Kalyanaraman B, and Sikora A**. Mechanism of oxidative conversion of Amplex® Red to resorufin: Pulse radiolysis and enzymatic studies. *Free Radic Biol Med* 95: 323-332, 2016.
14. **Dimauro I, Mercatelli N, and Caporossi D**. Exercise-induced ROS in heat shock proteins response. *Free Radic Biol Med* 98: 46-55, 2016.
15. **Done AJ, and Traustadóttir T**. Nrf2 mediates redox adaptations to exercise. *Redox biology* 10: 191-199, 2016.

16. **Drake JC, Wilson RJ, and Yan Z**. Molecular mechanisms for mitochondrial adaptation to exercise training in skeletal muscle. *The FASEB Journal* 30: 13-22, 2015.
17. **Dröse S, Brandt U, and Wittig I**. Mitochondrial respiratory chain complexes as sources and targets of thiol-based redox-regulation. *Biochimica et Biophysica Acta (BBA)-Proteins and Proteomics* 1844: 1344-1354, 2014.
18. **Egan B, Carson BP, Garcia-Roves PM, Chibalin AV, Sarsfield FM, Barron N, McCaffrey N, Moyna NM, Zierath JR, and O'Gorman DJ**. Exercise intensity-dependent regulation of peroxisome proliferator-activated receptor γ coactivator-1α mRNA abundance is associated with differential activation of upstream signalling kinases in human skeletal muscle. *J Physiol* 588: 1779-1790, 2010.
19. **Fisher-Wellman KH, and Neufer PD**. Linking mitochondrial bioenergetics to insulin resistance via redox biology. *Tr Endocr & Metab* 23: 142-153, 2012.
20. **Fu M-hH, Maher AC, Hamadeh MJ, Ye C, and Tarnopolsky MA**. Exercise, sex, menstrual cycle phase, and 17β-estradiol influence metabolism-related genes in human skeletal muscle. *Physiological genomics* 40: 34-47, 2009.
21. **Garber CE, Blissmer B, Deschenes MR, Franklin BA, Lamonte MJ, Lee I-M, Nieman DC, and Swain DP**. American College of Sports Medicine position stand. Quantity and quality of exercise for developing and maintaining cardiorespiratory, musculoskeletal, and neuromotor fitness in apparently healthy adults: guidance for prescribing exercise. *Medicine and science in sports and exercise* 43: 1334-1359, 2011.
22. **Gibala MJ, Little JP, Van Essen M, Wilkin GP, Burgomaster KA, Safdar A, Raha S, and Tarnopolsky MA**. Short-term sprint interval versus traditional endurance training: similar initial adaptations in human skeletal muscle and exercise performance. *J Physiol* 575: 901-911, 2006.
23. **Gill RM, O'Brien M, Young A, Gardiner D, and Mailloux RJ**. Protein S-glutathionylation lowers superoxide/hydrogen peroxide release from skeletal muscle mitochondria through modification of complex I and inhibition of pyruvate uptake. *PloS one* 13: e0192801, 2018.
24. **Goncalves RL, Quinlan CL, Perevoshchikova IV, Hey-Mogensen M, and Brand MD**. Sites of superoxide and hydrogen peroxide production by muscle mitochondria assessed ex vivo under conditions mimicking rest and exercise. *J Biol Chem* 290: 209-227, 2015.
25. **Granata C, Oliveira RS, Little JP, Renner K, and Bishop DJ**. Sprint-interval but not continuous exercise increases PGC-1α protein content and p53 phosphorylation in nuclear fractions of human skeletal muscle. *Scientific Reports* 7: 44227, 2017.
26. **Hawley J, and Noakes T**. Peak power output predicts maximal oxygen uptake and performance time in trained cyclists. *Eur J Appl Physiol Occup Physiol* 65: 79-83, 1992.
27. **Hickey AJR, Renshaw GMC, Speers-Roesch B, Richards JG, Wang Y, Farrell AP, and Brauner CJ**. A radical approach to beating hypoxia: depressed free radical release from heart fibres of the hypoxia-tolerant epaulette shark (Hemiscyllum ocellatum). *Journal of Comparative Physiology B: Biochemical, Systemic, and Environmental Physiology* 182: 91-100, 2011.
28. **Hüttemann M, Lee I, Samavati L, Yu H, and Doan JW**. Regulation of mitochondrial oxidative phosphorylation through cell signaling. *Biochimica et Biophysica Acta (BBA)-Molecular Cell Research* 1773: 1701-1720, 2007.
29. **Irrcher I, Ljubicic V, and Hood DA**. Interactions between ROS and AMP kinase activity in the regulation of PGC-1 transcription in skeletal muscle cells. *American Journal of Physiology-Cell Physiology* 296: C116, 2009.

30. **Jackson M**. Reactive oxygen species and redox-regulation of skeletal muscle adaptations to exercise. *Philosophical Transactions of the Royal Society of Biological Sciences* 360: 2285, 2005.
31. **Jackson MJ**. Redox regulation of muscle adaptations to contractile activity and aging. *J Appl Physiol* 119: 163-171, 2015.
32. **Kopprasch S, Srirangan D, Bergmann S, Graessler J, Schwarz PE, and Bornstein SR**. Association of systemic oxidative stress and insulin resistance/sensitivity indices–the PREDIAS study. *Clinical endocrinology* 2015.
33. **Kramer PA, Duan J, Qian W-J, and Marcinek DJ**. The Measurement of Reversible Redox Dependent Post-translational Modifications and Their Regulation of Mitochondrial and Skeletal Muscle Function. *Frontiers in physiology* 6: 347, 2015.
34. **Krumschnabel G, Fontana-Ayoub M, Sumbalova Z, Heidler J, Gauper K, Fasching M, and Gnaiger E**. Simultaneous high-resolution measurement of mitochondrial respiration and hydrogen peroxide production. *Mitochondrial Medicine: Volume I, Probing Mitochondrial Function* 245-261, 2015.
35. **Kruse R, Pedersen AJ, Kristensen JM, Petersson SJ, Wojtaszewski JF, and Højlund K**. Intact initiation of autophagy and mitochondrial fission by acute exercise in skeletal muscle of patients with Type 2 diabetes. *Clinical Science* 131: 37-47, 2017.
36. **Kubli DA, Quinsay MN, Huang C, Lee Y, and Gustafsson ÅB**. Bnip3 functions as a mitochondrial sensor of oxidative stress during myocardial ischemia and reperfusion. *American Journal of Physiology-Heart and Circulatory Physiology* 295: H2025-H2031, 2008.
37. **Leckey JJ, Hoffman NJ, Parr EB, Devlin BL, Trewin AJ, Stepto NK, Morton JP, Burke LM, and Hawley JA**. High dietary fat intake increases fat oxidation and reduces skeletal muscle mitochondrial respiration in trained humans. *The FASEB Journal* doi.org/10.1096/fj.201700993R: fj. 201700993R, 2018.
38. **Lee-Young RS, Canny BJ, Myers DE, and McConell GK**. AMPK activation is fiber type specific in human skeletal muscle: effects of exercise and short-term exercise training. *J Appl Physiol* 107: 283-289, 2009.
39. **Livak KJ, and Schmittgen TD**. Analysis of relative gene expression data using real-time quantitative PCR and the $2^{-\Delta\Delta CT}$ method. *Methods* 25: 402-408, 2001.
40. **MacInnis MJ, Zacharewicz E, Martin BJ, Haikalis ME, Skelly LE, Tarnopolsky MA, Murphy RM, and Gibala MJ**. Superior mitochondrial adaptations in human skeletal muscle after interval compared to continuous single-leg cycling matched for total work. *J Physiol* 595: 2955-2968, 2017.
41. **Mailloux RJ, and Harper ME**. Uncoupling proteins and the control of mitochondrial reactive oxygen species production. *Free Radic Biol Med* 51: 1106-1115, 2011.
42. **Mailloux RJ, Jin X, and Willmore WG**. Redox regulation of mitochondrial function with emphasis on cysteine oxidation reactions. *Redox biology* 2: 123-139, 2014.
43. **Mailloux RJ, Seifert EL, Bouillaud F, Aguer C, Collins S, and Harper ME**. Glutathionylation acts as a control switch for uncoupling proteins UCP2 and UCP3. *J Biol Chem* 286: 865-875, 2011.
44. **Milne KJ, and Noble EG**. Exercise-induced elevation of HSP70 is intensity dependent. *J Appl Physiol* 93: 561-568, 2002.
45. **Miwa S, Treumann A, Bell A, Vistoli G, Nelson G, Hay S, and von Zglinicki T**. Carboxylesterase converts Amplex Red to resorufin: implications for mitochondrial H 2 O 2 release assays. *Free Radic Biol Med* 90: 173-183, 2016.
46. **Murphy MP**. How mitochondria produce reactive oxygen species. *Biochemical Journal* 417: 1, 2009.

47. **Murphy RM, and Lamb GD**. Important considerations for protein analyses using antibody based techniques: down-sizing Western blotting up-sizes outcomes. *J Physiol* 591: 5823-5831, 2013.
48. **Nguyen T, Huang H, and Pickett CB**. Transcriptional regulation of the antioxidant response element Activation by Nrf2 and repression by MafK. *J Biol Chem* 275: 15466-15473, 2000.
49. **Parker L, Shaw C, Stepto NK, and Levinger I**. Exercise and Glycemic Control: Focus on Redox Homeostasis and Redox-Sensitive Protein Signaling. *Frontiers in Endocrinology* 8: 87, 2017.
50. **Parker L, Trewin A, Levinger I, Shaw CS, and Stepto NK**. Exercise-intensity dependent alterations in plasma redox status do not reflect skeletal muscle redox-sensitive protein signaling. *Journal of Science and Medicine in Sport* 2017.
51. **Parker L, Trewin AJ, Levinger I, Shaw CS, and Stepto NK**. The effect of exercise-intensity on skeletal muscle stress kinase and insulin protein signaling. *PLoS One* 12: e0171613, 2017.
52. **Picard M, Gentil BJ, McManus MJ, White K, Louis KS, Gartside SE, Wallace DC, and Turnbull DM**. Acute exercise remodels mitochondrial membrane interactions in mouse skeletal muscle. *J Appl Physiol* 115: 1562-1571, 2013.
53. **Powers S, Duarte J, Kavazis A, and Talbert E**. Reactive oxygen species are signalling molecules for skeletal muscle adaptation. *Experimental Physiology* 95: 1, 2010.
54. **Putman C, Jones N, Lands L, Bragg T, Hollidge-Horvat M, and Heigenhauser G**. Skeletal muscle pyruvate dehydrogenase activity during maximal exercise in humans. *Am J Physiol Endo Metab* 269: E458-E468, 1995.
55. **Sakellariou GK, Vasilaki A, Palomero J, Kayani A, Zibrik L, McArdle A, and Jackson MJ**. Studies of mitochondrial and nonmitochondrial sources implicate nicotinamide adenine dinucleotide phosphate oxidase (s) in the increased skeletal muscle superoxide generation that occurs during contractile activity. *Antioxidants & Redox Signaling* 18: 603-621, 2013.
56. **Salo DC, Donovan CM, and Davies KJ**. HSP70 and other possible heat shock or oxidative stress proteins are induced in skeletal muscle, heart, and liver during exercise. *Free Radic Biol Med* 11: 239-246, 1991.
57. **Scheele C, Nielsen S, and Pedersen BK**. ROS and myokines promote muscle adaptation to exercise. *Trends in Endocrinology & Metabolism* 20: 95-99, 2009.
58. **Smolka MB, Zoppi CC, Alves AA, Silveira LR, Marangoni S, Pereira-Da-Silva L, Novello JC, and Macedo DV**. HSP72 as a complementary protection against oxidative stress induced by exercise in the soleus muscle of rats. *American Journal of Physiology-Regulatory, Integrative and Comparative Physiology* 279: R1539-R1545, 2000.
59. **Song I-K, Lee J-J, Cho J-H, Jeong J, Shin D-H, and Lee K-J**. Degradation of redox-sensitive proteins including peroxiredoxins and DJ-1 is promoted by oxidation-induced conformational changes and ubiquitination. *Scientific reports* 6: 34432, 2016.
60. **Strobel NA, Matsumoto A, Peake JM, Marsh SA, Peternelj TT, Briskey D, Fassett RG, Coombes JS, and Wadley GD**. Altering the redox state of skeletal muscle by glutathione depletion increases the exercise-activation of PGC-1α. *Physiological reports* 2: e12224, 2014.
61. **Thompson JR, Swanson SA, Casale GP, Johanning JM, Papoutsi E, Koutakis P, Miserlis D, Zhu Z, and Pipinos II**. Gastrocnemius mitochondrial respiration: are there any differences between men and women? *Journal of Surgical Research* 185: 206-211, 2013.
62. **Timpani CA, Trewin AJ, Stojanovska V, Robinson A, Goodman CA, Nurgali K, Betik AC, Stepto N, Hayes A, and McConell GK**. Attempting to Compensate for Reduced

802 Neuronal Nitric Oxide Synthase Protein with Nitrate Supplementation Cannot Overcome
803 Metabolic Dysfunction but Rather Has Detrimental Effects in Dystrophin-Deficient mdx
804 Muscle. *Neurotherapeutics* 1-18, 2016.
805 63. **Tonkonogi M, Harris B, and Sahlin K**. Mitochondrial oxidative function in human
806 saponin-skinned muscle fibres: effects of prolonged exercise. *J Physiol* 510: 279-286, 1998.
807 64. **Tonkonogi M, Walsh B, Tiivel T, Saks V, and Sahlin K**. Mitochondrial function in
808 human skeletal muscle is not impaired by high intensity exercise. *Pflügers Archiv* 437: 562-
809 568, 1999.
810 65. **Trewin AJ, Berry BJ, and Wojtovich AP**. Exercise and Mitochondrial Dynamics:
811 Keeping in Shape with ROS and AMPK. *Antioxidants* 7: 7, 2018.
812 66. **Trewin AJ, Levinger I, Parker L, Shaw CS, Serpiello FR, Anderson MJ,**
813 **McConell GK, Hare DL, and Stepto NK**. Acute exercise alters skeletal muscle
814 mitochondrial respiration and H2O2 emission in response to hyperinsulinemic-euglycemic
815 clamp in middle-aged obese men. *PLoS One* 12: e0188421, 2017.
816 67. **Trewin AJ, Lundell LS, Perry BD, Patil KV, Chibalin AV, Levinger I, McQuade**
817 **LR, and Stepto NK**. Effect of N-acetylcysteine infusion on exercise induced modulation of
818 insulin sensitivity, and signaling pathways in human skeletal muscle. *Am J Physiol Endo*
819 *Metab* 309: E388-397, 2015.
820 68. **Vainshtein A, Tryon LD, Pauly M, and Hood DA**. Role of PGC-1α during acute
821 exercise-induced autophagy and mitophagy in skeletal muscle. *American Journal of*
822 *Physiology-Cell Physiology* 308: C710-C719, 2015.
823 69. **Votion DM, Fraipont A, Goachet A-G, Robert C, van Erck E, Amory H,**
824 **Ceusters J, de la Rebière de Pouyade G, Franck T, and Mouithys-Mickalad A**.
825 Alterations in mitochondrial respiratory function in response to endurance training and
826 endurance racing. *Equine Veterinary Journal* 42: 268-274, 2010.
827 70. **Wadley AJ, Aldred S, and Coles SJ**. An unexplored role for Peroxiredoxin in
828 exercise-induced redox signalling? *Redox biology* 8: 51-58, 2016.
829 71. **Wadley GD, Nicolas MA, Hiam D, and McConell GK**. Xanthine oxidase inhibition
830 attenuates skeletal muscle signaling following acute exercise but does not impair
831 mitochondrial adaptations to endurance training. *Am J Physiol Endo Metab* 304: E853-E862,
832 2013.
833 72. **Wang L, Psilander N, Tonkonogi M, Ding S, and Sahlin K**. Similar expression of
834 oxidative genes after interval and continuous exercise. *Med Sci Sports Exerc* 41: 2136-2144,
835 2009.
836 73. **Westerblad H, Bruton JD, and Katz A**. Skeletal muscle: energy metabolism, fiber
837 types, fatigue and adaptability. *Experimental cell research* 316: 3093-3099, 2010.
838 74. **Wong H-S, Dighe PA, Mezera V, Monternier P-A, and Brand MD**. Production of
839 superoxide and hydrogen peroxide from specific mitochondrial sites under different
840 bioenergetic conditions. *J Biol Chem* 292: 16804-16809, 2017.
841 75. **Zhang J, and Ney PA**. Role of BNIP3 and NIX in cell death, autophagy, and
842 mitophagy. *Cell Death & Differentiation* 16: 939-946, 2009.
843

844

845 **Table 1: List of primer sequences for real-time PCR**

Gene	NCBI RefSeq	Forward primer 5' - 3'	Reverse primer 5' - 3'
β-2M	NM_004048.2	TGCTGTCTCCATGTTTGATGTATCT	TCTCTGCTCCCCACCTCTAAGT
BNIP3	NM_004052.3	TGGACGGAGTAGCTCCAAGA	AAAGAGGAACTCCTTGGGGG
DRP1	NM_012062.4	CACCCGGAGACCTCTCATTC	CCCCATTCTTCTGCTTCCAC
GPX1	NM_000581.2	CGCCACCGCGCTTATGACCG	GCAGCACTGCAACTGCCAAGCAG
MFN2	NM_014874.3	CCCCCTTGTCTTTATGCTGATGTT	TTTTGGGAGAGGTGTTGCTTATTTC
NFE2L2	NM_006164.4	AAGTGACAAGATGGGCTGCT	TGGACCACTGTATGGGATCA
PPARGC1A	NM_013261.3	GGCAGAAGGCAATTGAAGAG	TCAAAACGGTCCCTCAGTTC
PRDX1	NM_001202431.1	CCCAACTTCAAAGCCACAGC	AAAGGCCCCTGAACGAGATG
SOD1	NM_000454.4	GGTCCTCACTTTAATCCTCTAT	CATCTTTGTCAGCAGTCACATT
SOD2	NM_001024465.1	CTGGACAAACCTCAGCCCTA	TGATGGCTTCCAGCAACTC
TXNRD1	NM_003330.3	AGCATGTCATGTGAGGACGG	AGAGTCTTGCAGGGCTTGTC
UCP3	NM_003356.3	CCACAGCCTTCTACAAGGGATTTA	ACGAACATCACCACGTTCCA

846
847 Abbreviations: *β-2M*, β_2 microglobulin; *BNIP3*, BCL2/adenovirus E1B 19kDa interacting protein 3; *DRP1*,
848 Dynamin 1-like protein; *GPX1*, Glutathione peroxidase-1; *MFN2*, Mitofusin-2; *NFE2L2*, Nuclear factor
849 erythroid 2-related factor 2; *PPARGC1A*, Peroxisome proliferator-activated receptor gamma, coactivator 1
850 alpha; *PRDX1*, Peroxiredoxin-1; *SOD1*, Cytosolic superoxide dismutase 1; *SOD2*, Mitochondrial manganese
851 superoxide dismutase; *TXNRD1*, Thioredoxin reductase 1; *UCP3*, Uncoupling protein-3.
852

Table 2: Physiological demands and responses to acute exercise protocols

	CMIE	HIIE	SIE
Total exercise session time incl. rest periods (min)	30 ± 0[bc]	24 ± 0[ac]	15 ± 0[ab]
Exercise time (min)	30 ± 0[bc]	20 ± 0[ac]	2 ± 0[ab]
Mean power output (Watts)	163 ± 36[bc]	245 ± 54[ac]	645 ± 71[ab]
Total mechanical work (kJ)	294 ± 65[c]	294 ± 65[c]	76 ± 14[ab]
Intensity (% PPO)	50 ± 0[bc]	75 ± 0[ac]	198 ± 25[ab]
Intensity (% $\dot{V}O_{2peak}$)	54 ± 3[bc]	77 ± 1[ac]	-
HR, session peak (bpm)	158 ± 15[b]	182 ± 11[ac]	168 ± 9[b]
RPE, session peak (AU)	13 ± 2[bc]	18 ± 1[ac]	20 ± 0[ab]

CMIE, continuous moderate intensity exercise; HIIE, high intensity interval exercise; SIE, sprint interval exercise; RPE, rating of perceived exertion (6-20). Data are mean ± SD, n=8. [a]$p<0.05$, compared to CMIE; [b]$p<0.05$, compared to HIIE; [c]$p<0.05$, compared to SIE.

Figure legends

Figure 1. Mitochondrial respiration from permeabilized human skeletal muscle fibers.
(A) Representative mitochondrial oxygen flux (JO_2) trace depicts one sample in a single chamber from a baseline condition. Light gray line (left y-axis) is chamber O_2 concentration, dark line (right y-axis) is mitochondrial O_2 consumption (JO_2) rate throughout the substrate inhibitor uncoupled titration (SUIT) protocol. Various respiratory states were induced as follows: (B) state-4 leak (*LEAK*) supported by complex-I substrates malate and pyruvate, (C) addition of succinate for complex-II, (D) ADP (5 mM) stimulated state-3 (*OXPHOS*) and (E) uncoupled (*ETS*) states with complexes I+II substrate input or (F) complex-II only after rotenone complex-I inhibition. Muscle samples were taken at baseline (BASE), immediately after exercise (EX) and after 3 hours recovery (3HR). CMIE, continuous moderate intensity exercise; HIIE, high intensity interval exercise; SIE, sprint interval exercise; *ww*, wet-weight muscle. Data are mean ± SD, for n=8. Main time effect p<0.05: #compared to BASE, †compared to EX.

Figure 2. Mitochondrial H_2O_2 emission from permeabilized human muscle fibers.
(A) Representative mitochondrial hydrogen peroxide trace depicts one sample in a single chamber from a baseline condition. Light gray line (left y-axis) is cumulative Amplex UltraRed fluorescent reaction product in the chamber proportional to H_2O_2 formation, dark line (right y-axis) is H_2O_2 emission rate (JH_2O_2) throughout the substrate inhibitor uncoupled titration (SUIT) protocol used to induce various respiratory states: (B) state-4 leak (*LEAK*) supported by complex-I substrates malate and pyruvate, (C) addition of succinate for complex-II. (D) ADP (5 mM) stimulated state-3 (*OXPHOS*) and (E) uncoupled (ETS) states with complexes I+II substrate input or (F) complex-II only after rotenone complex-I inhibition. Muscle samples were taken at baseline (BASE), immediately after exercise (EX) and after 3 hours recovery (3HR). CMIE, continuous moderate intensity exercise; HIIE, high intensity interval exercise; SIE, sprint interval exercise; *ww*, wet-weight muscle. Data are mean ± SD, for n=8. Main time effect p<0.05 unless otherwise stated: #compared to BASE, †compared to EX.

Figure 3. Muscle protein phosphorylation responses to exercise.
Representative western blots (A) of phosphorylated acetyl-coA carboxylase at serine 221 (B), AMP activated protein kinase at threonine 172 (C) and heat shock protein of 27 kDa serine 82 (D); before (BASE), immediately (EX) and 3 hours (3HR) after continuous moderate intensity (CMIE), high intensity interval (HIIE) and sprint interval exercise (SIE). Representative blots are from a single participants' samples. Blot densitometry was normalized to stain-free total protein, and quantified relative to standard curves generated on each membrane (not shown). Data are mean ± SD, n=8. Main time effect p<0.05 unless otherwise stated: #compared to BASE, †compared to EX.

Figure 4. mRNA expression of genes associated with mitochondrial biogenesis, morphology and mitophagy (A), and redox homeostasis (B) 3h after the different exercise bouts.
Muscle mRNA expression analysed by qPCR is fold-change normalized to a housekeeping gene, β2-microglobulin (β-2M) at 3 hours post exercise relative to respective baseline (depicted by dashed line). CMIE, continuous moderate intensity exercise; HIIE, high intensity interval exercise; SIE, sprint interval exercise. Data are mean ± SD, n=8. Main time effect across all exercise protocols: # p<0.05 compared to baseline.

Figure 5. Proteins involved in redox homeostasis and mitochondrial function.
(A) Representative western blots. Blots were quantified for antioxidant proteins (B) peroxiredoxin, (C) thioredoxin, (D) glutathione peroxidase-1, and (E) thioredoxin reductase-1; mitochondrial morphology proteins (F) mitofusin-2 and (G) dynamin-related protein-1; mitochondrial proteins (H) peroxisome proliferator-activated receptor gamma coactivator 1-alpha, (I) uncoupling protein 3 and (J) mitochondrial transcription factor A; and (K) heat-shock protein of 72 kDa. Blot densitometry was normalized to stain-free total protein, and quantified relative to internal calibration curves on each membrane. Exercise was continuous moderate intensity (CMIE), high intensity interval (HIIE) and sprint interval (SIE) exercise, samples obtained at baseline (BASE), immediately post exercise (EX) and after 3 h recovery (3HR). Representative blots are shown from one subject. Data are mean ± SD, n=8. Main time effect $p<0.05$ unless otherwise stated: #compared to BASE, †compared to EX. *$p<0.05$ exercise intensity effect.

Figure 6: Mitochondrial complex I – V protein abundance.
Subunits of complex I (NDUFB8), II (SDHB), III (UQRCR2), IV subunit 2 (MTCO2), IV subunit 4 (COX-IV) and V (ATP5A) were assessed by Western blot (A-F, respectively). Exercise was continuous moderate intensity (CMIE), high intensity interval (HIIE) and sprint interval (SIE) exercise, samples obtained at baseline (BASE), immediately post exercise (EX) and after 3 h recovery (3HR). Blot densitometry was normalized to stain-free total protein, and quantified relative to internal calibration curves on each membrane. Representative blots are shown from one subject. Data are mean ± SD, n=8.

Figure 7: Mitochondrial protein S-glutathionylation.
Protein (50 µg) from whole muscle lysate was co-immunoprecipitated with anti-GSH antibody on sepharose beads, then detected via Western blot, as per *methods*. Representative images show mitochondrial complexes V (ATP5A), IV subunit 2 (MTCO2), and UCP-3 from one subject at each time point (A) and co-IP pull-down was confirmed on the same membrane using a negative control in the absence of anti-GSH antibody in the pull-down (No-IP), along with whole muscle lysate as positive control (lysate) (B). Protein S-glutathionylation was expressed relative to each respective baseline level of protein glutathionylation (C-E). Exercise was continuous moderate intensity (CMIE), high intensity interval (HIIE) and sprint interval (SIE) exercise, samples obtained at baseline (BASE), immediately post exercise (EX) and after 3 h recovery (3HR). Data are mean ± SD for n=3-4.

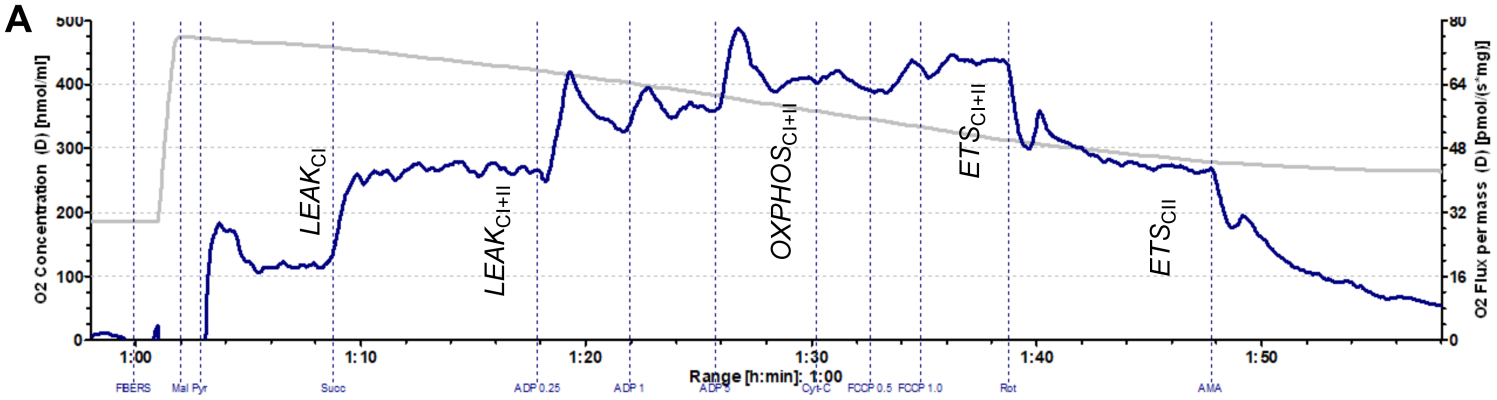
A
O2 Concentration (D) [nmol/ml]
O2 Flux per mass (D) [pmol/(s*mg)]
LEAK_CI
LEAK_CI+II
OXPHOS_CI+II
ETS_CI+II
ETS_CII
1:00
1:10
1:20
1:30
1:40
1:50
Range [h:min]: 1:00
FBERS
Mal Pyr
Succ
ADP 0.25
ADP 1
ADP 5
Cyt-C
FCCP 0.5
FCCP 1.0
Rot
AMA

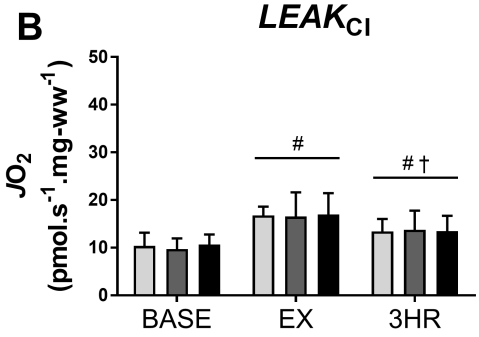
B
LEAK_CI
JO2 (pmol.s-1.mg-ww-1)
#
#†
BASE
EX
3HR

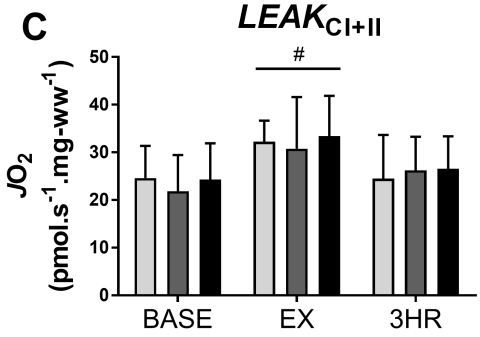
C
LEAK_CI+II
JO2 (pmol.s-1.mg-ww-1)
#
BASE
EX
3HR


CMIE
HIIE
SIE

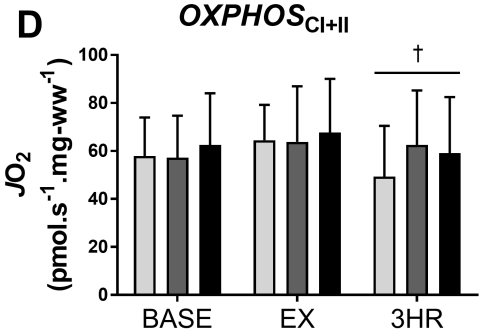
D
OXPHOS_CI+II
JO2 (pmol.s-1.mg-ww-1)
†
BASE
EX
3HR

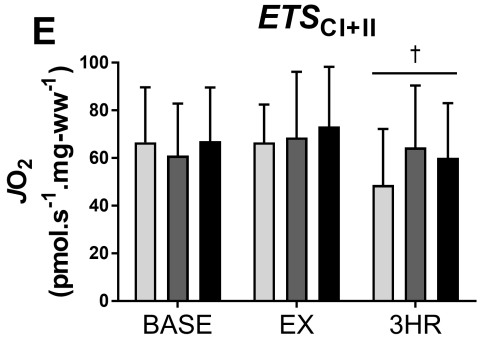
E
ETS_CI+II
JO2 (pmol.s-1.mg-ww-1)
†
BASE
EX
3HR

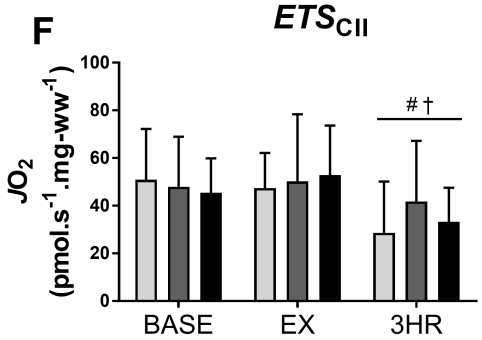
F
ETS_CII
JO2 (pmol.s-1.mg-ww-1)
#†
BASE
EX
3HR

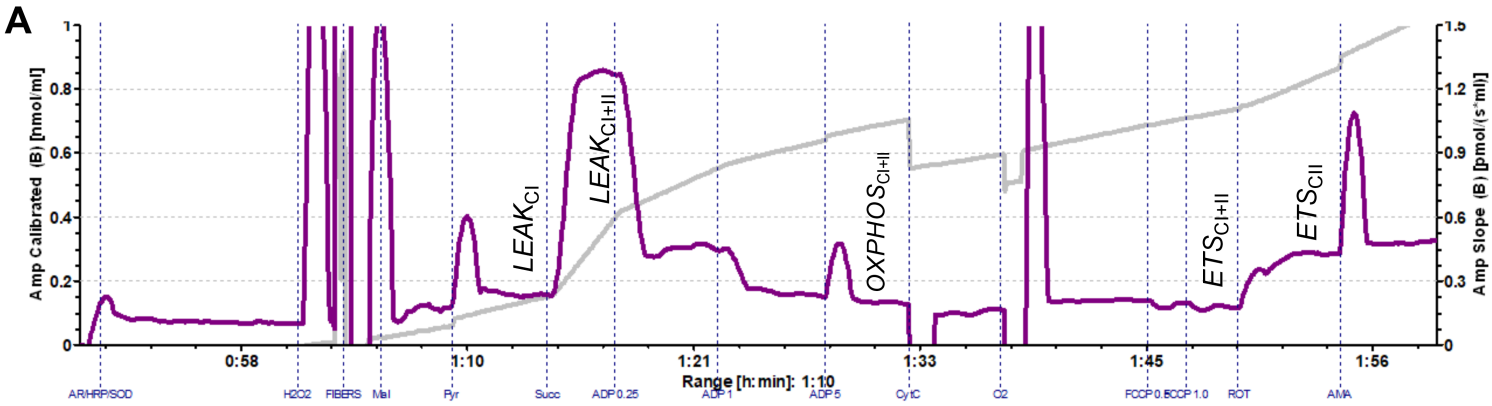
A
Amp Calibrated (B) [nmol/ml]
Amp Slope (B) [pmol/(s*ml)]
LEAK_CI
LEAK_CI+II
OXPHOS_CI+II
ETS_CI+II
ETS_CII
0:58
1:10
1:21
1:33
1:45
1:56
Range [h:min]: 1:10
AR
HRP
SOD
H2O2
FIBERS
Mal
Pyr
Succ
ADP 0.25
ADP 1
ADP 5
CytC
O2
FCCP 0.5
FCCP 1.0
ROT
AMA

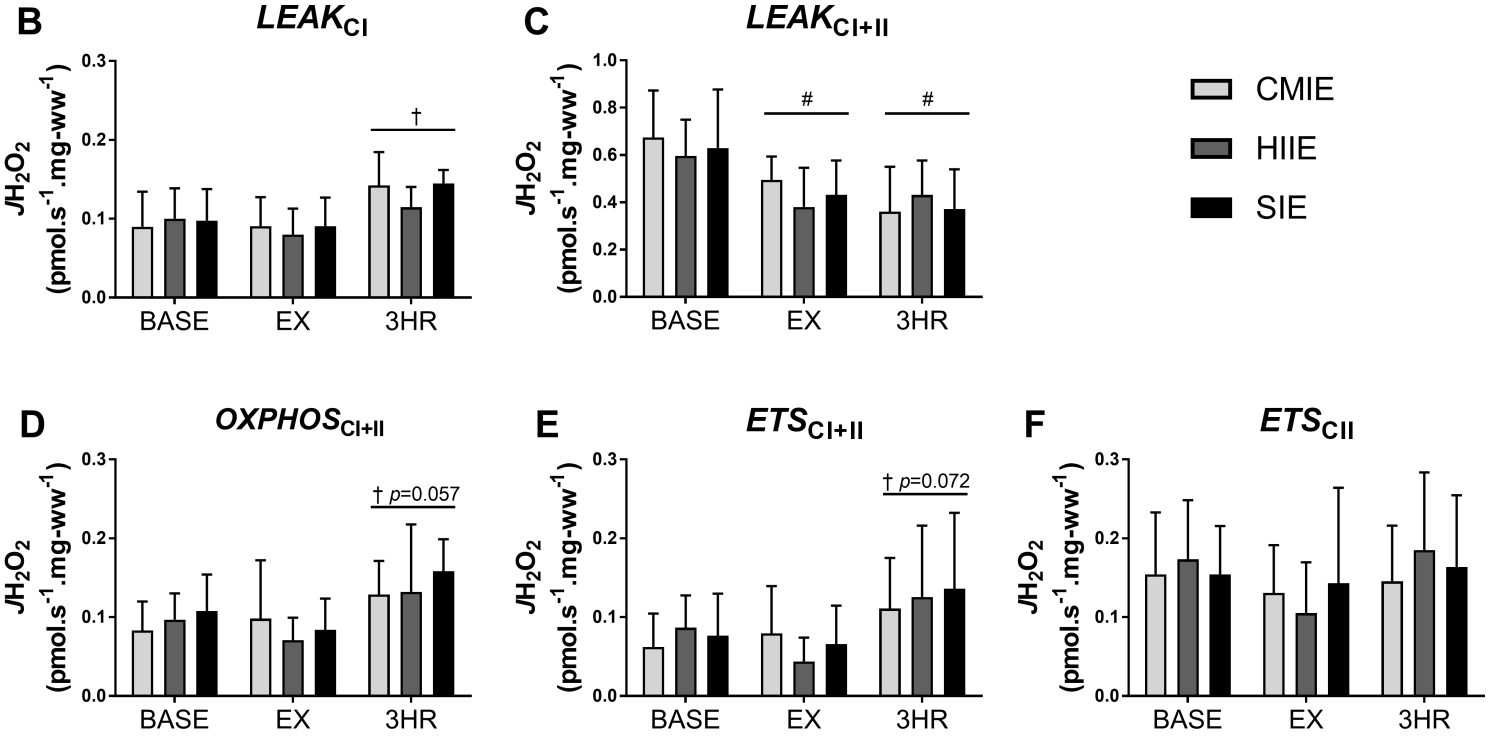
B
LEAK_CI
C
LEAK_CI+II
D
OXPHOS_CI+II
E
ETS_CI+II
F
ETS_CII
JH2O2 (pmol.s-1.mg-ww-1)
BASE
EX
3HR
†
#
† p=0.057
† p=0.072
CMIE
HIIE
SIE

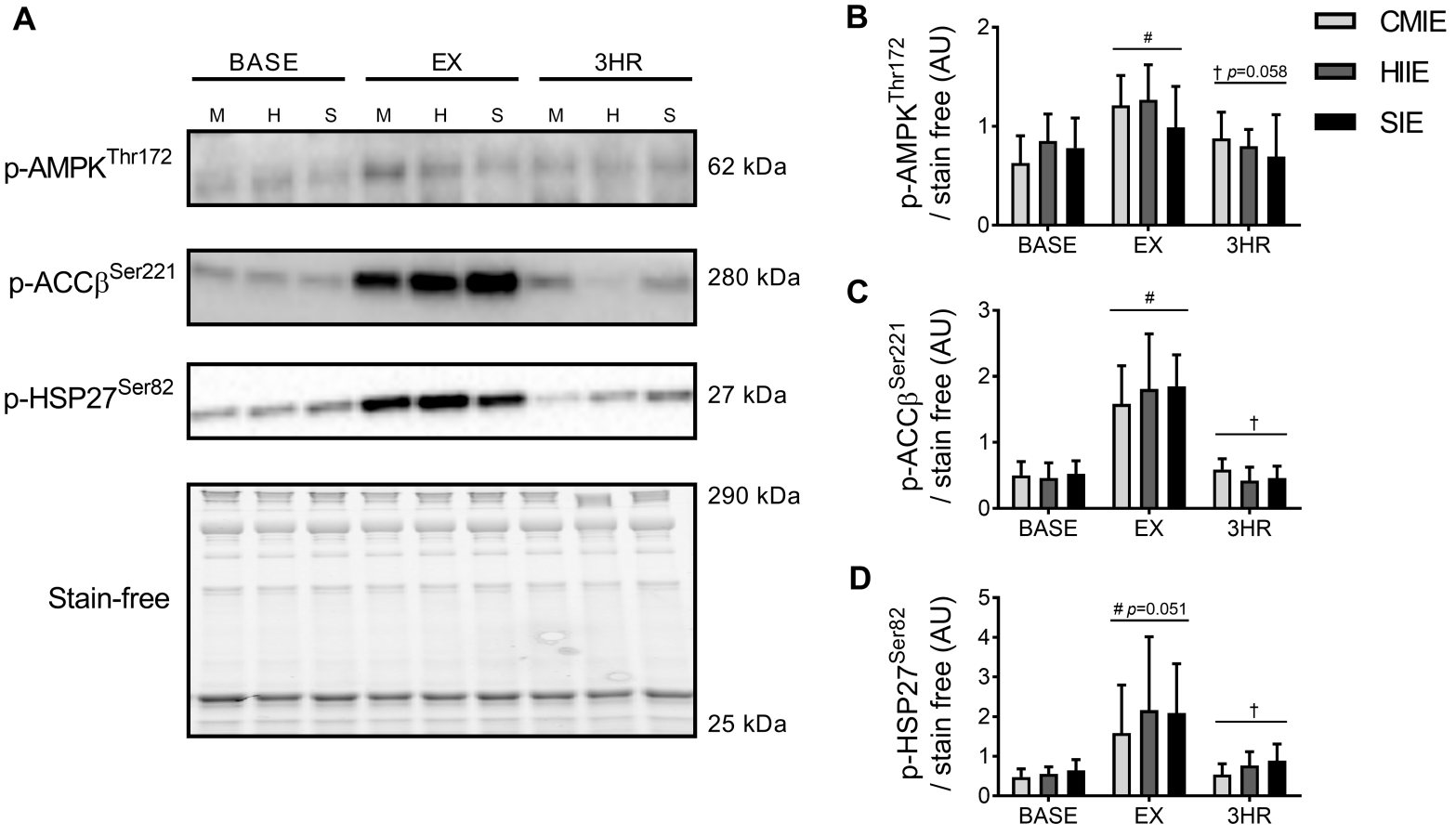
A
BASE
EX
3HR
M H S M H S M H S
p-AMPK^Thr172
62 kDa
p-ACCβ^Ser221
280 kDa
p-HSP27^Ser82
27 kDa
290 kDa
Stain-free
25 kDa
B
p-AMPK^Thr172 / stain free (AU)
#
† p=0.058
CMIE
HIIE
SIE
BASE
EX
3HR
C
p-ACCβ^Ser221 / stain free (AU)
#
†
D
p-HSP27^Ser82 / stain free (AU)
p=0.051
†

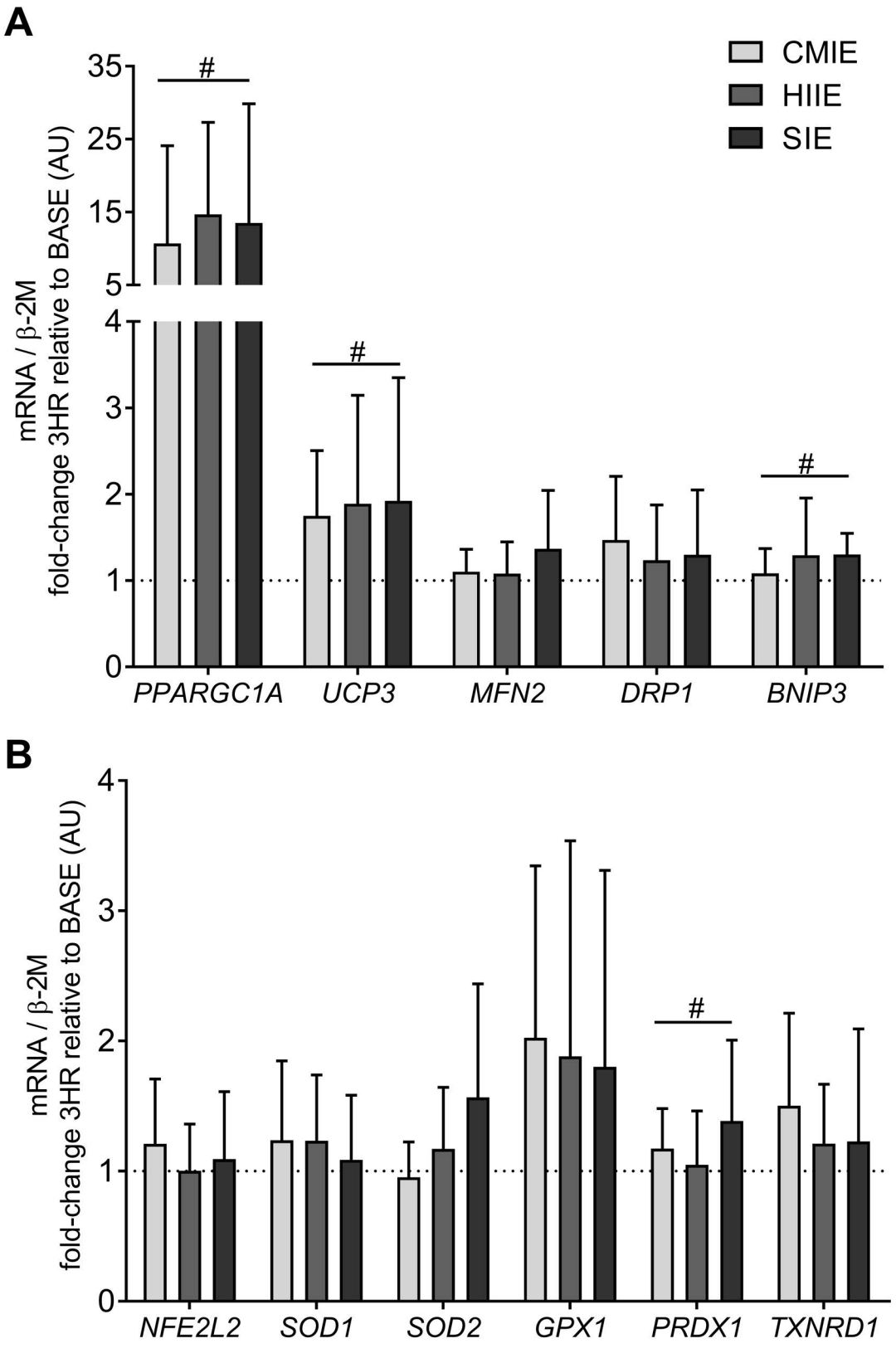
A
CMIE
HIIE
SIE
mRNA / β-2M
fold-change 3HR relative to BASE (AU)
35
25
15
5
4
3
2
1
0
#
#
#
PPARGC1A
UCP3
MFN2
DRP1
BNIP3
B
mRNA / β-2M
fold-change 3HR relative to BASE (AU)
4
3
2
1
0
#
NFE2L2
SOD1
SOD2
GPX1
PRDX1
TXNRD1

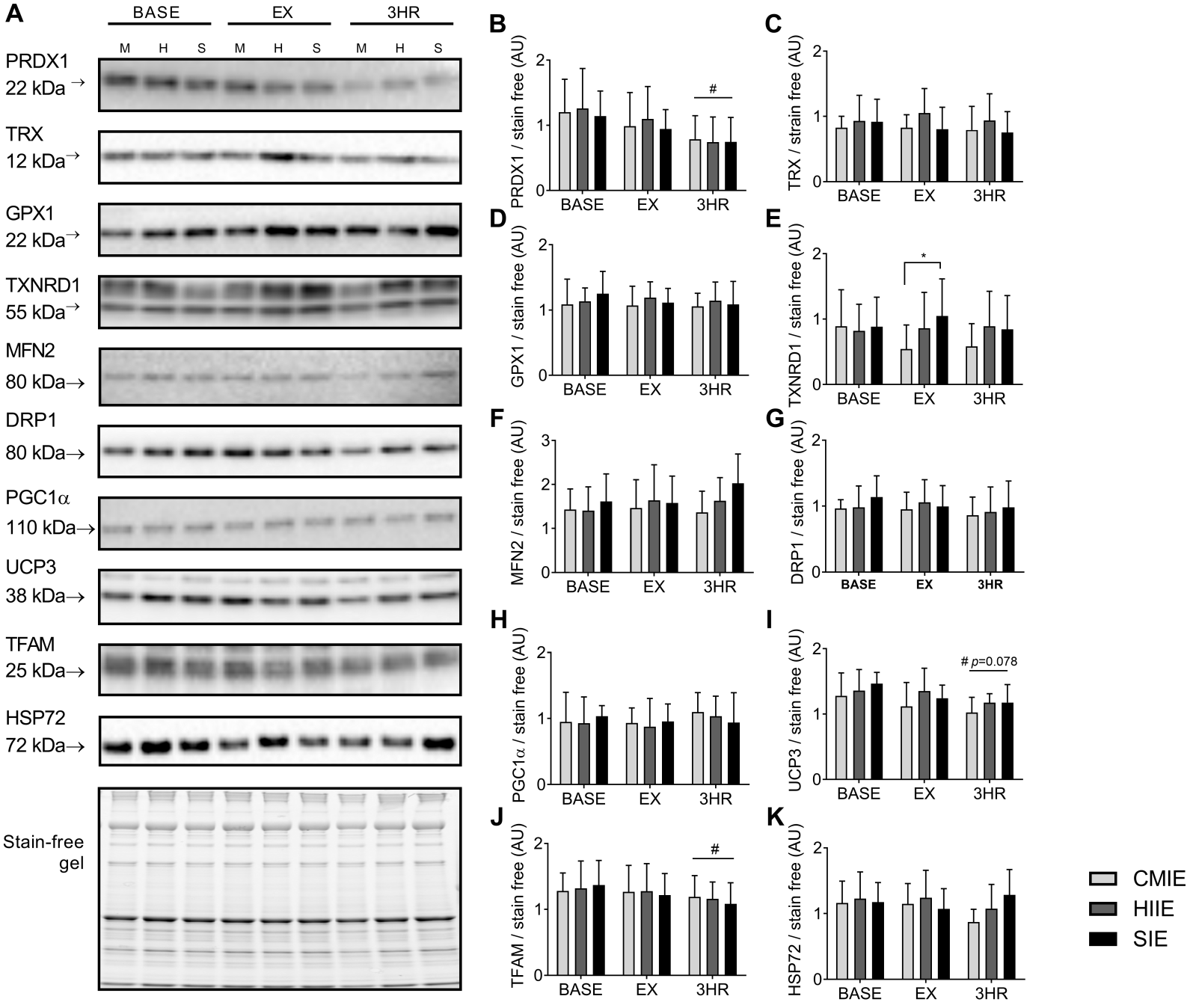
A
BASE
EX
3HR
M H S M H S M H S
PRDX1
22 kDa →
TRX
12 kDa→
GPX1
22 kDa→
TXNRD1
55 kDa→
MFN2
80 kDa→
DRP1
80 kDa→
PGC1α
110 kDa→
UCP3
38 kDa→
TFAM
25 kDa→
HSP72
72 kDa→
Stain-free gel
B
PRDX1 / stain free (AU)
C
TRX / strain free (AU)
D
GPX1 / stain free (AU)
E
TXNRD1 / stain free (AU)
F
MFN2 / stain free (AU)
G
DRP1 / stain free (AU)
H
PGC1α / stain free (AU)
I
UCP3 / stain free (AU)
p=0.078
J
TFAM / stain free (AU)
K
HSP72 / stain free (AU)
BASE
EX
3HR
CMIE
HIIE
SIE

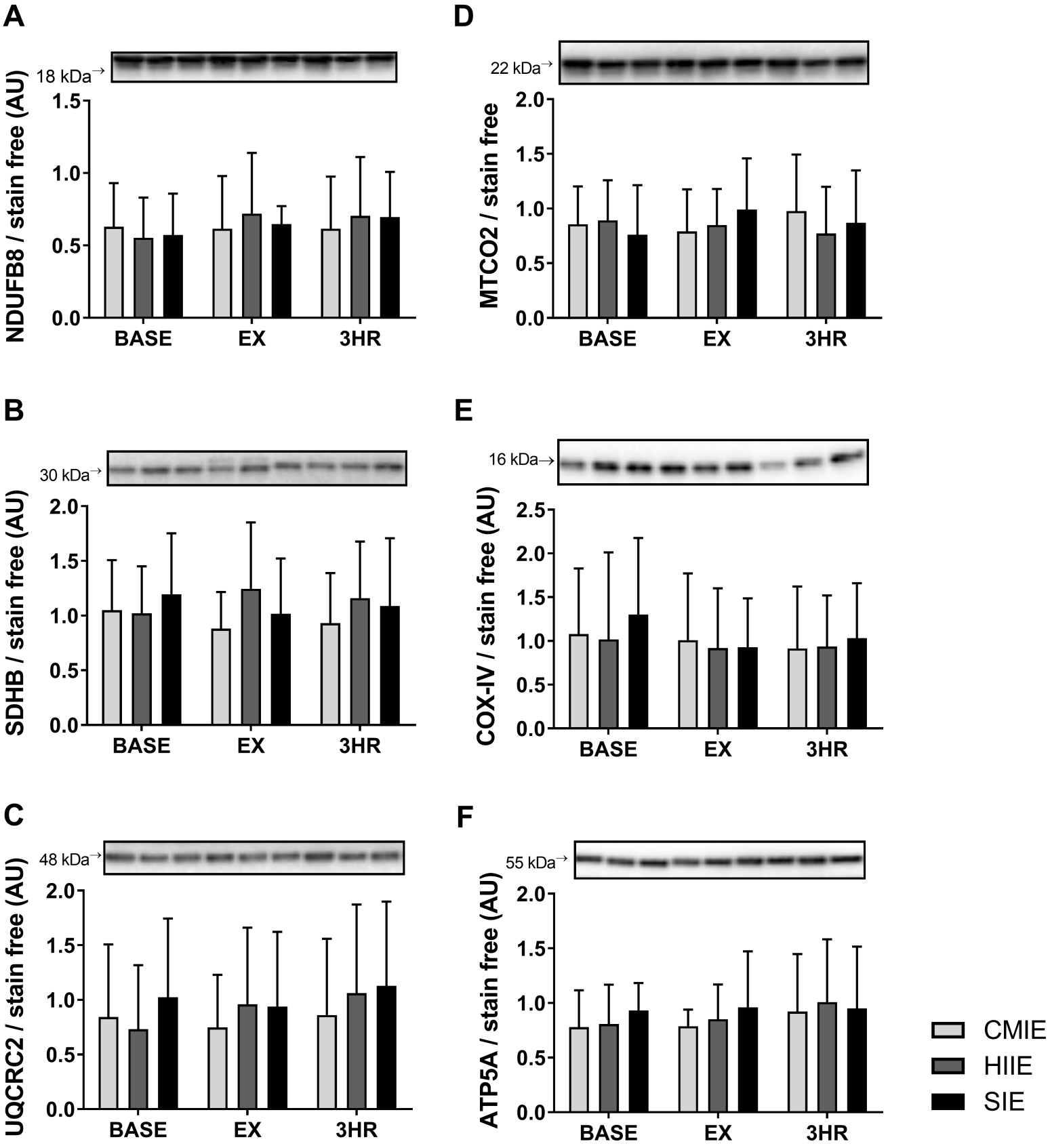
A
18 kDa→
NDUFB8 / stain free (AU)
1.5
1.0
0.5
0.0
BASE
EX
3HR
D
22 kDa→
MTCO2 / stain free
2.0
1.5
1.0
0.5
0.0
BASE
EX
3HR
B
30 kDa→
SDHB / stain free (AU)
2.0
1.5
1.0
0.5
0.0
BASE
EX
3HR
E
16 kDa→
COX-IV / stain free (AU)
2.5
2.0
1.5
1.0
0.5
0.0
BASE
EX
3HR
C
48 kDa→
UQCRC2 / stain free (AU)
2.0
1.5
1.0
0.5
0.0
BASE
EX
3HR
F
55 kDa→
ATP5A / stain free (AU)
2.0
1.5
1.0
0.5
0.0
BASE
EX
3HR
CMIE
HIIE
SIE

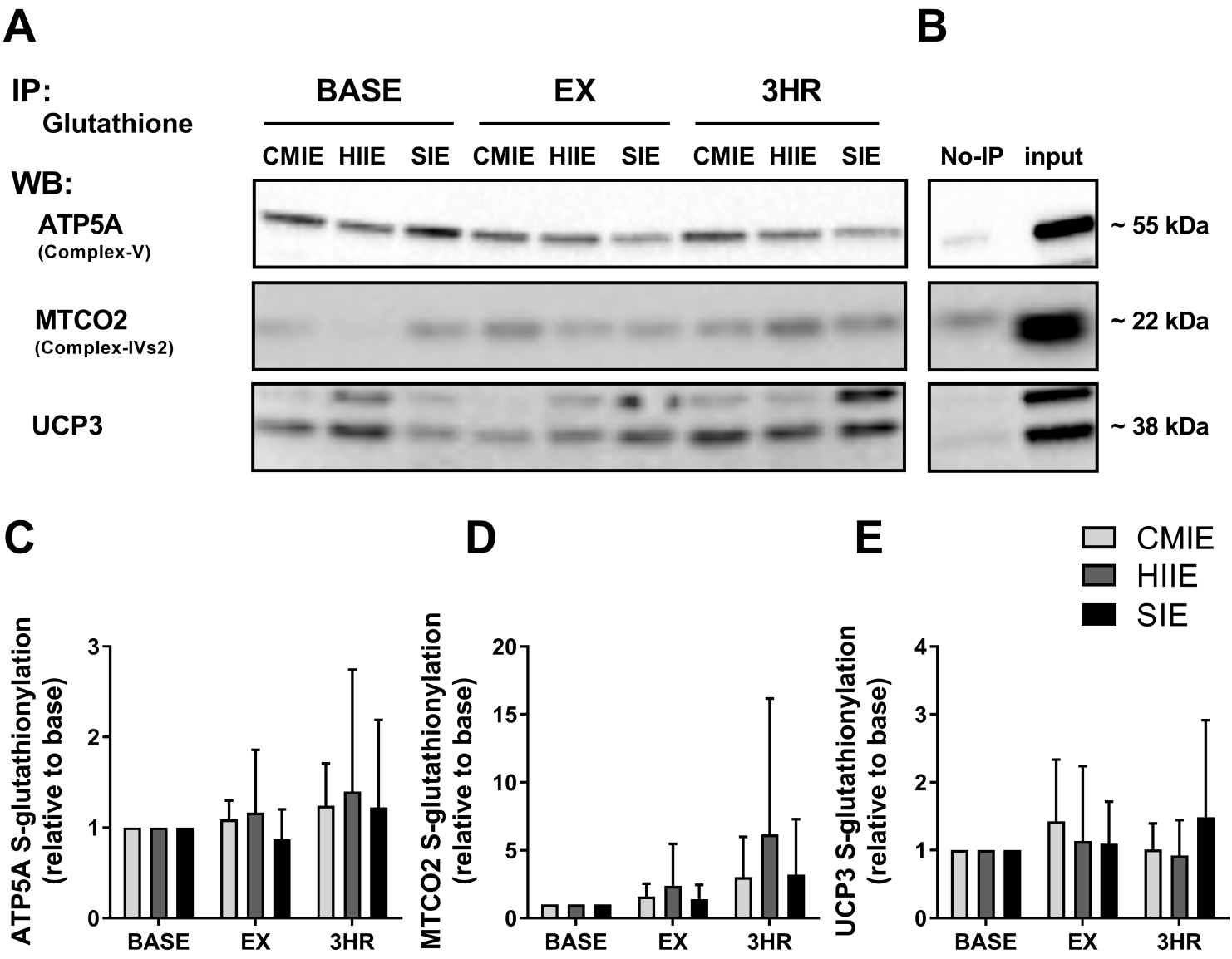
A
B
IP:
Glutathione
BASE
EX
3HR
CMIE HIIE SIE CMIE HIIE SIE CMIE HIIE SIE
No-IP input
WB:
ATP5A
(Complex-V)
MTCO2
(Complex-IVs2)
UCP3
~ 55 kDa
~ 22 kDa
~ 38 kDa
C
D
E
CMIE
HIIE
SIE
ATP5A S-glutathionylation (relative to base)
MTCO2 S-glutathionylation (relative to base)
UCP3 S-glutathionylation (relative to base)
BASE
EX
3HR